

# Generating quantum matrix geometry from gauged quantum mechanics

Kazuki Hasebe

*National Institute of Technology, Sendai College, Ayashi, Sendai, 989-3128, Japan*

 (Received 5 October 2023; accepted 28 November 2023; published 27 December 2023)

Quantum matrix geometry is the underlying geometry of M(atr)ix theory. Expanding upon the idea of level projection, we propose a quantum-oriented noncommutative scheme for generating the matrix geometry of the coset space  $G/H$ . We employ this novel scheme to unveil unexplored matrix geometries by utilizing gauged quantum mechanics on higher dimensional spheres. The resultant matrix geometries manifest as pure quantum Nambu geometries: Their noncommutative structures elude capture through the conventional commutator formalism of Lie algebra, necessitating the introduction of the quantum Nambu algebra. This matrix geometry embodies a one-dimension-lower quantum internal geometry featuring nested fuzzy structures. While the continuum limit of this quantum geometry is represented by overlapping classical manifolds, their fuzzification cannot reproduce the original quantum geometry. We demonstrate how these quantum Nambu geometries give rise to novel solutions in Yang-Mills matrix models, exhibiting distinct physical properties from the known fuzzy sphere solutions.

DOI: [10.1103/PhysRevD.108.126023](https://doi.org/10.1103/PhysRevD.108.126023)

## I. INTRODUCTION

It has been almost 80 years since the inception of theoretical research on quantized space-time with Snyder's first explicit model [1,2]. This research field continues to be active, contributing to a deeper understanding of space-time. Noncommutative geometry presents a promising mathematical framework for describing the microscopic nature of space-time [3]. A general mathematical framework of noncommutative geometry was set up by Connes [4]. More tangible noncommutative schemes are those such as deformation quantization, geometric quantization, and Berezin-Toeplitz quantization [5]. As these ideas are rooted in the canonical quantization method of the phase space [6,7], the corresponding noncommutative schemes are concerned with the quantization of the symplectic manifolds or Poisson manifolds. However, in the investigations of M theory, physicists encountered even exotic noncommutative structures beyond the conventional quantization schemes, including odd dimensional fuzzy spheres [8–11]. From M(atr)ix theory point of view [12,13], matrix geometries known as fuzzy manifolds [14–26] represent fundamental extended objects in the theory [27,28]. Moreover, it has been recognized that the quantum Nambu algebra [29] plays crucial roles in the formulation of M theory (see Refs. [30–32] as nice reviews

and references therein). It may be evident that a new noncommutative scheme is required to address these extraordinary noncommutative spaces that extend beyond the conventional quantization methods based on the commutator formalism.<sup>1</sup>

Associated with the developments of the higher-dimensional quantum Hall effect, the understanding of higher-dimensional noncommutative geometry has significantly advanced in the past 20 years (see [39,40] and references therein). We have learned that the higher dimensional noncommutative geometry on  $\mathcal{M} \simeq G/H$  can be obtained by examining the Landau model on  $\mathcal{M}$  in the non-Abelian monopole background [41–52]. Specifically, within the lowest Landau level, fuzzy manifolds  $\mathcal{M}_F$  were successfully realized. Nonetheless, it should be noticed that the underlying reason for the success is still missing. Furthermore, while the preceding analysis has provided a nice physical understanding of noncommutative geometries, one could argue that these analyses have not revealed unknown matrix geometries. Until now, substantial attention has been given to the geometry in the lowest Landau level; however, there is no logical reason for the exclusive presence of noncommutative geometry solely in this level. Indeed, it was demonstrated that the higher Landau levels also give rise to fuzzy geometries [53], which clearly shows that level projection to any Landau level generates

---

*Published by the American Physical Society under the terms of the Creative Commons Attribution 4.0 International license. Further distribution of this work must maintain attribution to the author(s) and the published article's title, journal citation, and DOI. Funded by SCOAP<sup>3</sup>.*

---

<sup>1</sup>Interestingly, a cubit matrix realization is known for the quantum Nambu algebra [33–35], although we do not delve into such possibilities in this paper. The deformation quantization approach to the quantum Nambu geometry is also discussed in Refs. [36–38].

noncommutativity. With regards to a two-sphere, the emergent noncommutative geometries of the higher Landau levels are the same as that of the lowest Landau level. In this sense, the geometry of higher Landau levels might not be so intriguing. Nevertheless, this does not rule out the possibility of discovering new noncommutative geometries in higher dimensional systems. Following this idea, explorations of novel quantum matrix geometries have been conducted in various Landau models, such as relativistic models and supersymmetric models [53], odd dimensional models [54] and even dimensional models [55–57]. It is also worthwhile to mention that quantum matrix geometries associated with the Berezin-Toeplitz quantization have been intensively studied in recent years [58–64].

Importantly, now the higher dimensional studies are not only relevant to theoretical interests but also to practical experiments. The idea of the synthetic dimension allows physicists to reach higher dimensional topological physics [65–67]. In particular, exotic topological effects of the non-Abelian monopole in higher dimension have already been observed through table top experiments very recently [68–71]. It is expected that physical consequences arising from higher dimensional quantum geometry will be observed in these experimental systems.

In the present work, with an appropriate interpretation of the emergent noncommutative geometry in the Landau models, we introduce a quantum-oriented noncommutative scheme that leverages Landau models as an effective “tool” to generate noble quantum geometries. Our approach provides a concrete prescription for generating the matrix geometry of the coset manifold  $\mathcal{M} \simeq G/H$ . It is shown that this scheme encompasses pure quantum Nambu matrix geometry, which cannot be described by conventional noncommutative methods. We also demonstrate that these quantum Nambu matrix geometries give rise to novel classical solutions in Yang-Mills matrix models.

This paper is organized as follows. In Sec. II, we revisit the derivation of the fuzzy two-sphere from the  $SO(3)$  Landau model and address the underlying reasons behind the emergent noncommutative geometry of the Landau models. Section III presents explicit fuzzy four-sphere matrix coordinates in the  $SO(5)$  Landau levels. We investigate the matrix structures of fuzzy four-spheres and discuss their basic properties in Sec. IV. In Sec. V, the nested internal structures of higher Landau level matrix geometries are exploited. We investigate the continuum limit and the classical geometry of the quantum matrix geometry using the coherent method and the probe brane method in Sec. VI. In Sec. VII, we demonstrate that the obtained quantum matrix geometries realize unexplored solutions of Yang-Mills matrix models and clarify their physical properties. Section IX is devoted to summary and discussions.

## II. QUANTUM-ORIENTED NONCOMMUTATIVE SCHEME

In this section, we discuss the underlying mechanism behind the emergent matrix geometry in the simple  $SO(3)$  Landau model and apply this observation to propose a prescription for generating matrix geometries of  $G/H$ .

### A. Behind the scene of the emergent matrix geometry

The  $SO(3)$  Landau model is a Landau model on  $S^2$  and the Hamiltonian is given by

$$H = -\frac{1}{2M} \sum_{i=1}^3 (\partial_i + iA_i)^2|_{r=1}, \quad (1)$$

where  $A_i$  denotes the  $U(1)$  gauge field of monopole at the origin:

$$A_i = -\frac{I}{2r(r+x_3)} \epsilon_{ij3} x_j. \quad (2)$$

The index  $I/2$  signifies the monopole charge (in the following, we assume  $I$  to be a positive integer for simplicity). While the present system is originally investigated in [72,73], we will utilize the concise notation of [53] in this paper. The eigenvalues of the Hamiltonian (1) are obtained as

$$E_N = \frac{1}{2M} \left( I \left( N + \frac{1}{2} \right) + N(N+1) \right) \quad (N = 0, 1, 2, \dots), \quad (3)$$

and the corresponding eigenstates are given by the monopole harmonics

$$Y_m^{(N)}(\theta, \phi) = \sqrt{\frac{2N+I+1}{4\pi}} \mathcal{D}_{N+\frac{1}{2}}(\phi, -\theta, -\phi)_{\frac{1}{2}, m} \left( m = N + \frac{I}{2}, N + \frac{I}{2} - 1, \dots, -\left( N + \frac{I}{2} \right) \right), \quad (4)$$

where  $\mathcal{D}$  denotes the Wigner D function:

$$\mathcal{D}_l(\chi, \theta, \phi) = e^{-i\chi S_z^{(l)}} e^{-i\theta S_y^{(l)}} e^{-i\phi S_z^{(l)}}. \quad (5)$$

Here,  $S_i^{(l)}$  stand for the  $SU(2)$  spin matrices with spin index  $l$ . We sandwich the coordinates on  $S^2$  to derive the corresponding matrix coordinates:

$$(X_i^{(N)})_{mn} = \langle Y_m^{(N)} | x_i | Y_n^{(N)} \rangle \equiv \int_{S^2} d\theta d\phi \sin \theta Y_m^{(N)*} x_i Y_n^{(N)}, \quad (6)$$

where

$$x_1 = \cos \phi \sin \theta, \quad x_2 = \sin \phi \sin \theta, \quad x_3 = \cos \theta. \quad (7)$$

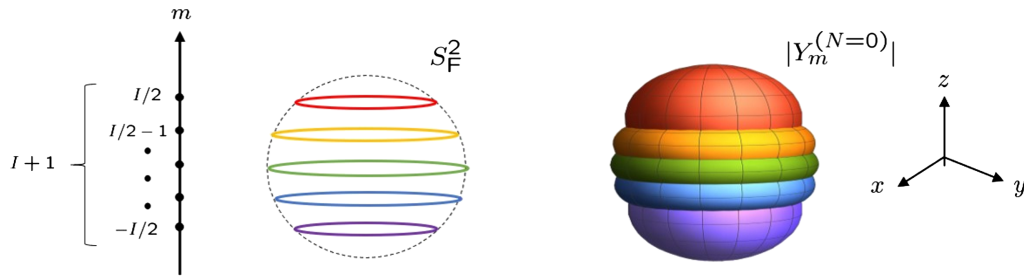


FIG. 1. Left: the schematic picture of the fuzzy two-sphere for  $N = 0$  (8). Right: the distributions of the magnitudes of the monopole harmonics,  $|Y_m^{(N=0)}|$ , of  $m = I/2, I/2 - 1, \dots, -I/2$  for  $I = 4$  are depicted as the red, orange, green, blue, and violet orbitals, respectively. The monopole orbitals,  $|Y_m^{(N=0)}|$ , are localized around the latitudes  $z = 2m/I$  on the two-sphere.

In the  $N$ th Landau level,  $X_i^{[N]}$  are explicitly obtained as [53]

$$X_i^{(N)} = \frac{2I}{(I+2N)(I+2N+2)} S_i^{(\frac{I}{2}+N)}, \quad (8)$$

which satisfy

$$X_i^{(N)} X_i^{(N)} = \frac{I^2}{(I+2N)(I+2N+2)} \mathbf{1}_{I+2N+1}, \quad (9a)$$

$$[X_i^{(N)}, X_j^{(N)}] = i \frac{2I}{(I+2N)(I+2N+2)} \epsilon_{ijk} X_k^{(N)}. \quad (9b)$$

Equation (9) represents the algebra of fuzzy two-sphere [14]. Note that not only the lowest Landau level but also each of the higher Landau level matrix geometries realizes the fuzzy two-sphere matrix geometry.<sup>2</sup> The physical properties of (9) as a classical solution of Yang-Mills matrix models are discussed in Appendix B.

We depicted the fuzzy two-sphere and the magnitudes of the monopole harmonics in the left and the right of Fig. 1, respectively. One may find an apparent resemblance between the left and the right pictures. The latitudes on the fuzzy two-sphere represent the degrees of freedom of the matrix geometry, i.e., the “points,” in the fuzzy space. Obviously, each point on the fuzzy space corresponds to the monopole harmonics or each state of the  $SU(2)$  irreducible representation. Therefore, one may consider the fuzzy two-sphere to be composed of the  $SU(2)$  irreducible representation.

Reflecting the emergence of the noncommutative geometry, we can obtain the following insight:

- (1) About the role of global symmetry and irreducible representation: The  $SO(3)$  global symmetry of  $S^2 \simeq SO(3)/SO(2)$  is naturally transformed to the  $SU(2)$  symmetry on the matrix geometry side introducing the projective representation of  $SO(3)$ . In the matrix geometry, an “uncertainty area” or a “point” corre-

sponds to each state of the  $SU(2)$  irreducible representation. The irreducible representation is “symmetric” in the sense that, while each state of an irreducible representation is transformed, the set of states in the irreducible representation remains unchanged under any  $SU(2)$  transformation. In the language of matrix geometry, this means that fuzzy geometry also remains unchanged under  $SU(2)$  transformations, as the fuzzy two-sphere is composed of the states in the  $SU(2)$  irreducible representation. Moreover, the  $SU(2)$  group is a compact group, and its irreducible representation is a finite-dimensional set with discrete quantum numbers, which aligns with the intuitive notion that a compact noncommutative space consists of finite-dimensional discrete points. In this way, while the fuzzy sphere is a discretized space, it realizes a space symmetric under continuous  $SU(2)$  transformations, unlike the lattice space, which is symmetric only by the discrete translations corresponding to the lattice spacing. This is the specific feature of the matrix geometry composed of the irreducible representation.

- (2) About the role of the stabilizer group and the gauge symmetry: The stabilizer group  $SO(2)$  of  $S^2 \simeq SO(3)/SO(2)$  is a subgroup of  $SO(3)$  that does not change a point on the classical manifold  $S^2$  [74]. A point in the classical geometry corresponds to a state of the irreducible representation on the matrix geometry side. Therefore, the stabilizer group is considered to be some transformation that does not change that state. The transformation that does not change physical state is nothing but a gauge transformation. To encapsulate, the stabilizer group represents redundant symmetry of the  $SO(3)$  group in the classical system when representing  $S^2 \simeq SO(3)/SO(2)$ , and such redundancy is naturally regarded as a gauge symmetry on the quantum mechanical side. Consequently, the stabilizer group  $SO(2)$  corresponds to the  $U(1) \simeq SO(2)$  symmetry on the quantum mechanical side. It is interesting to see that while the stabilizer symmetry is an external symmetry on the classical mechanical side,

<sup>2</sup>For completeness, we derive the noncommutative geometry in higher Landau levels of the planar Landau model in Appendix A.

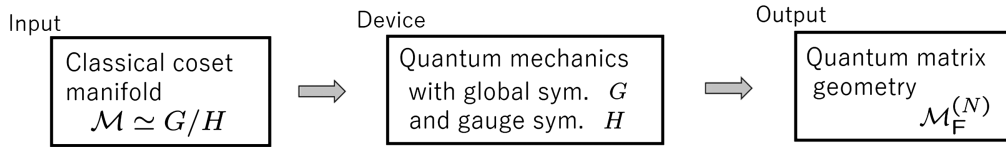


FIG. 2. Flow of the procedure.

it acts as the internal symmetry on the quantum mechanical side.<sup>3</sup>

- (3) Reinterpretation of the Landau model: The above observations suggest that the matrix geometry corresponding to  $S^2 \simeq SO(3)/SO(2)$  is obtained by considering a quantum system with global  $SU(2)$  symmetry and  $U(1)$  gauge symmetry. As we are dealing with the spatial manifold, the  $U(1)$  gauge symmetry introduces the  $U(1)$  vector potential whose field configuration should be compatible with the  $SU(2)$  global symmetry. This necessarily leads to the radially symmetric magnetic field of the  $U(1)$  monopole. Thus, the magnetic field is just a consequence of the gauge symmetry. In this way, we can reproduce the original  $SO(3)$  Landau system. It is important to note that the primary significance lies in the gauge symmetry itself rather than the magnetic field, although the presence of a magnetic field is commonly believed to be essential for the emergence of noncommutative geometry.

These speculations provide a natural explanation for why the fuzzy two-sphere geometry has been successfully generated through the analyses of the  $SO(3)$  Landau model.

## B. Noncommutative scheme for generating the matrix geometry

With the above understanding, we now propose a prescription for obtaining the matrix geometry of the general coset manifold,  $\mathcal{M} \simeq G/H$ . We will utilize the quantum mechanics as a tool for generating matrix geometries. What we need to do is simply replace the  $SO(3)$  in the above discussions with  $G$  and  $SO(2)$  with  $H$ .<sup>4</sup>

### 1. General prescription

- (1) Consider quantum mechanics with gauge symmetry  $H$  on base-manifold  $\mathcal{M}$ :

$$-\frac{1}{2M} \sum_a D_a^2 \Big|_{\mathcal{M}}, \quad (10)$$

<sup>3</sup>This suggests that the external space and the internal space should be treated on the same footing in the matrix geometry [75].

<sup>4</sup>While we will assume that  $G$  is a compact group with finite dimensional irreducible representations, our discussions can also be applied to noncompact groups with discrete series of infinite dimensional irreducible representations [26].

where  $D_a = \partial_a + iA_a$  are covariant derivatives with the gauge field  $A_a$  of the gauge group  $H$ . The gauge field configuration has to be chosen to be compatible with the symmetry  $G$  of the base-manifold  $\mathcal{M}$ .

- (2) Solve the eigenvalue problem of the Hamiltonian (10) to derive the degenerate eigenstates of each energy level  $E_N$ :

$$|\psi_{N,\alpha}\rangle. \quad (11)$$

The set of degenerate eigenstates constitute an irreducible representation of  $G$ .<sup>5</sup>

- (3) Derive the matrix elements of the coordinates  $x_a$  of  $\mathcal{M}$  utilizing (11) to construct the matrix coordinates of  $\mathcal{M}_F^{(N)}$ :

$$(X_a^{(N)})_{\alpha\beta} = \langle \psi_{N,\alpha} | x_a | \psi_{N,\beta} \rangle \equiv \int_{\mathcal{M}} d\Omega \psi_{N,\alpha}^\dagger x_a \psi_{N,\beta}, \quad (12)$$

where  $d\Omega$  is the area element of  $\mathcal{M}$ .

Notice each energy level  $N$  hosts its own matrix geometry  $X_a^{(N)}$ , and distinct energy levels yield different quantum matrix coordinates in general. Consequently, multiple quantum geometries will be obtained from a single classical manifold. The flow of this procedure is depicted in Fig. 2.

### 2. Advantages

Here, we will outline the advantages of the present construction.

- (1) The first merit is that we do not need to worry about mathematical inconsistency. In the present scheme, noncommutative geometry is not postulated *a priori* but is what emerges in each of the energy levels. As the original quantum system is totally physical and the existence of mathematically consistent Hilbert space behind the quantum mechanics is founded, there is no need to be concerned about mathematical inconsistencies.<sup>6</sup>
- (2) Following the above simple prescription, we can mechanically derive matrix geometries for arbitrary

<sup>5</sup>In general, the Hamiltonian may possess symmetries other than  $G$ . In such a case, the degenerate eigenstates constitute states of an irreducible representation of the entire symmetry. See Sec. VB.

<sup>6</sup>This is inspired by the idea of Ref. [76].

classical manifolds of the type  $\mathcal{M} \simeq G/H$ . Notably, odd dimensional manifolds are also within the realm of this scheme. Therefore, this scheme is not restricted to the symplectic manifolds unlike the conventional quantization methods in which the quantization is basically executed by replacing the Poisson bracket with the commutator. This suggests that the present scheme is beyond the noncommutative geometry based on the canonical commutator formalism.

- (3) The present noncommutative scheme is primarily based on irreducible representations of quantum mechanics. In this sense, this may be referred to as a quantum-oriented scheme. The emergent matrix geometries may even encompass pure quantum geometries that do not have their classical counterparts. We may explore quantum geometries that have eluded in the conventional noncommutative schemes.

### C. General properties

To examine specific properties of the present scheme, let us consider even dimensional spheres:

$$S^{2k} \simeq SO(2k+1)/SO(2k). \quad (13)$$

#### 1. Covariance

We assume that the global symmetry  $SO(2k+1)$  of  $S^{2k}$  is given by

$$x_{a=1,2,\dots,2k+1} \rightarrow R_{ab}x_b \quad (R_{ab} \in SO(2k+1)). \quad (14)$$

The stabilizer group is defined so that the condition  $x_a = \delta_{a,2k+1}$  does not change, which is the  $SO(2k)$  transformation:

$$x_{\mu=1,2,\dots,2k} \rightarrow R_{\mu\nu}x_\nu \quad (R_{\mu\nu} \in SO(2k)). \quad (15)$$

Transformations (14) and (15), respectively, correspond to the following transformations on the quantum mechanics side:

$$|\psi_\alpha^{(i)}\rangle \rightarrow |\psi_\beta^{(i)}\rangle U_{\beta\alpha} \quad (U \in \text{Spin}(2k+1)), \quad (16)$$

and

$$|\psi_\alpha^{(i)}\rangle \rightarrow g_{ij}|\psi_\alpha^{(j)}\rangle \quad (g \in \text{Spin}(2k)). \quad (17)$$

Equation (16) stands for the global transformation, and  $\alpha$  denote the index of the irreducible representation of the  $\text{Spin}(2k+1)$ . Similarly, Eq. (17) represents the gauge

transformation, and  $i$  signify that of the gauge group  $\text{Spin}(2k)$ . Under these transformations,  $X_a$  behave as

$$\begin{aligned} (X_a)_{\alpha\beta} &= \sum_i \langle \psi_\alpha^{(i)} | x_a | \psi_\beta^{(i)} \rangle \rightarrow \sum_i U_{\alpha'\alpha}^* \langle \psi_{\alpha'}^{(i)} | x_a | \psi_\beta^{(i)} \rangle U_{\beta'\beta} \\ &= (U^\dagger X_a U)_{\alpha\beta} = R_{ab} (X_b)_{\alpha\beta}, \end{aligned} \quad (18)$$

and

$$\begin{aligned} (X_a)_{\alpha\beta} &= \sum_i \langle \psi_\alpha^{(i)} | x_a | \psi_\beta^{(i)} \rangle \rightarrow \sum_{j,k} \sum_i \overbrace{g_{ij}^* g_{ik}}^{=\delta_{jk}} \langle \psi_\alpha^{(j)} | x_a | \psi_\beta^{(k)} \rangle \\ &= \sum_j \langle \psi_\alpha^{(j)} | x_a | \psi_\beta^{(j)} \rangle = (X_a)_{\alpha\beta}. \end{aligned} \quad (19)$$

The matrix coordinates thus transform as the  $SO(2k+1)$  vector, similar to the classical coordinates on  $S^{2k}$ , and they are gauge invariant. Generally for  $\mathcal{M} \simeq G/H$ , the matrix coordinates are  $H$  gauge invariant and transform under  $G$  in the same way as the classical coordinates of the original manifold  $\mathcal{M}$ .

#### 2. Beyond the commutator formalism

In the well known construction of the fuzzy  $2k$ -sphere [15,16], the matrix coordinates are given by the totally symmetric combination of the gamma matrices, which satisfy the following commutation relations

$$[X_a, X_b] = 4i\Sigma_{ab}, \quad (20a)$$

$$[X_a, \Sigma_{bc}] = -i\delta_{ab}X_c + i\delta_{ac}X_b, \quad (20b)$$

$$[\Sigma_{ab}, \Sigma_{cd}] = i\delta_{ac}\Sigma_{bd} - i\delta_{ad}\Sigma_{bc} + i\delta_{bd}\Sigma_{ac} - i\delta_{bc}\Sigma_{ad}. \quad (20c)$$

The commutators of  $X_a$  yield new matrices  $\Sigma_{ab}$  (20a), which are the generators of  $SO(2k+1)$ . In total,  $X_a$  and  $\Sigma_{ab}$  together form the  $SO(2k+2)$  algebra. Such a matrix geometry is known to emerge in the lowest Landau level of the  $SO(2k+1)$  Landau model [75]. The lowest Landau level matrix geometry is well described by the commutator formalism. On the other hand, for the higher Landau levels, some subtleties occur. The  $SO(2k+1)$  angular momentum operators in the  $SO(2k)$  monopole background are constructed as [44]

$$L_{ab} = -ix_a(\partial_b + iA_b) + ix_b(\partial_a + iA_a) + \frac{1}{r^2}F_{ab}, \quad (21)$$

which satisfy the  $SO(2k+1)$  algebra:

$$[L_{ab}, L_{cd}] = i\delta_{ac}L_{bd} - i\delta_{ad}L_{bc} + i\delta_{bd}L_{ac} - i\delta_{bc}L_{ad}. \quad (22)$$

Since the coordinates  $x_a$  on  $S^{2k}$  transform as an  $SO(2k+1)$  vector, the algebra associated with the  $SO(2k+1)$  transformation is represented as

$$[x_a, L_{bc}] = -i\delta_{ab}x_c + i\delta_{ac}x_b. \quad (23)$$

Let us construct matrix coordinates for a given irreducible representation of  $SO(2k+1)$ ,  $\{\psi_1^{(r)}, \psi_2^{(r)}, \dots, \psi_{D(r)}^{(r)}\}$ :

$$(X_a^{(r)})_{\alpha\beta} \equiv \langle \psi_\alpha^{(r)} | x_a | \psi_\beta^{(r)} \rangle, \quad (\Sigma_{ab}^{(r)})_{\alpha\beta} \equiv \langle \psi_\alpha^{(r)} | L_{ab} | \psi_\beta^{(r)} \rangle. \quad (24)$$

It is important to note that the completeness relation holds for the total set of the irreducible representations:

$$\sum_r \sum_{\alpha=1}^{D(r)} |\psi_\alpha^{(r)}\rangle \langle \psi_\alpha^{(r)}| = 1, \quad (25)$$

but not for each individual irreducible representation:

$$\sum_{\alpha=1}^{D(r)} |\psi_\alpha^{(r)}\rangle \langle \psi_\alpha^{(r)}| \neq 1. \quad (26)$$

Equation (26) is a direct consequence of the level projection which is the heart of noncommutative geometry [53]. Due to Eq. (26),  $X_a^{(r)}$  (24) generally become noncommutative matrices, whereas the original coordinates  $x_a$  are commutative quantities. From the property of the irreducible representation

$$\langle \psi_\alpha^{(r)} | L_{ab} | \psi_\beta^{(r')} \rangle = (\Sigma_{ab}^{(r)})_{\alpha\beta} \delta_{rr'}, \quad (27)$$

one may easily reproduce the lower two equations of (20) using Eqs. (22) and (23). On the other hand, unlike Eq. (27), the matrix coordinates are not completely block diagonalized,  $\langle \psi_\alpha^{(r)} | x_a | \psi_\beta^{(r')} \rangle \neq \langle \psi_\alpha^{(r)} | x_a | \psi_\beta^{(r)} \rangle \delta_{rr'}$  (see Sec. III A for more details). Consequently, the first relation (20a) turns out to be questionable,

$$[X_a^{(r)}, X_b^{(r)}] \stackrel{?}{\propto} i\Sigma_{ab}^{(r)}. \quad (28)$$

Equation (20a) is not guaranteed in general. So, if the Lie algebraic geometry fails, what kind of geometry will emerge? That is the topic that we shall discuss in Secs. IV and VIII. The failure of Eq. (20a) implies that the present scheme is beyond the realm of the conventional commutator formalism.

Here, we also mention relationship to the Berezin-Toeplitz quantization. The Berezin-Toeplitz quantization is a method that maps a function to a finite dimensional matrix [5,62,77]. In this sense, the Berezin-Toeplitz quantization shares the same spirit with the present scheme.

However, Berezin-Toeplitz quantization is primarily concerned with symplectic manifolds and is based on commutator formalism. The Kernel employed in the Berezin-Toeplitz quantization corresponds to the zero modes of the Dirac-Landau operator whose zero modes are essentially equivalent to the lowest Landau level eigenstates [53,55]. Therefore, the Berezin-Toeplitz quantization is thus closely related to the lowest Landau level matrix geometry and can be viewed as a special case of the present scheme.<sup>7</sup> We will revisit this in Sec. IV.

### III. MATRIX COORDINATES FROM THE $SO(5)$ LANDAU MODEL

In this section, we will directly apply the present scheme to generate quantum matrix geometries for  $S^4$ . Using the  $SO(5)$  Landau model, we will derive the complete form of matrix coordinates in arbitrary Landau levels. This section also includes a review of Ref. [55].

#### A. The $SO(5)$ Landau model

Since  $S^4 \simeq SO(5)/SO(4)$ , we need to consider a quantum mechanics on  $S^4$  with Spin(4) gauge degrees of freedom. For the Spin(4) gauge field configuration to respect the  $SO(5)$  global symmetry of  $S^4$ , we place a Spin(4) monopole at the origin. While the Landau model in such a Spin(4) monopole background has been investigated [57], we will consider a simpler system by taking one  $SU(2)$  from the Spin(4)  $\simeq SU(2) \otimes SU(2)$ . In the following, we then consider a quantum mechanics on  $S^4$  in the  $SU(2)$  monopole background, which was originally introduced in Refs. [41,80,81].

Let us briefly discuss such a  $SO(5)$  Landau model with a modern notation [55]. The  $SO(5)$  Landau Hamiltonian is given by

$$H = -\frac{1}{2M} \sum_{a=1}^5 D_a^2 |_{r=0} = \frac{1}{2M} \sum_{a<b} \Lambda_{ab}^2, \quad (29)$$

where  $D_a = \partial_a + iA_a$  and

$$\Lambda_{ab} = -ix_a D_b + ix_b D_a. \quad (30)$$

The gauge field is chosen to be Yang's  $SU(2)$  monopole:

$$A_{\mu=1,2,3,4} = -\frac{1}{r(r+x_5)} \bar{\eta}_{\mu\nu}^i x_\nu S_i^{(I/2)}, \quad A_5 = 0, \quad (I = 1, 2, 3, \dots), \quad (31)$$

with  $\bar{\eta}_{\mu\nu}^i = \epsilon_{\mu\nu i 4} - \delta_{\mu i} \delta_{\nu 4} + \delta_{\nu i} \delta_{\mu 4}$ . The  $SO(5)$  Landau Hamiltonian is equal to the  $SO(5)$  Casimir up to a constant.

<sup>7</sup>Recently mathematicians are also interested in higher Landau levels from the perspective of the Berezin-Toeplitz quantization [78,79].

Consequently, the energy eigenvalues are specified by two indices of the  $SO(5)$  Casimir,  $(p, q)_5 = (N + I, N)_5$ . The  $SO(5)$  Landau levels are explicitly given by

$$E_N = \frac{1}{2M} ((N + 1)I + N(N + 3)) \quad (N = 0, 1, 2, \dots). \quad (32)$$

The eigenstates of each of the Landau levels form an irreducible representation of  $SO(5)$  and are referred to as the  $SO(5)$  monopole harmonics in this paper<sup>8</sup> to emphasize its  $SO(5)$  covariance. We parametrize the coordinates of the four-sphere with a unit radius as

$$x_{\mu=1,2,3,4} = \sin \xi y_{\mu}, \quad x_5 = \cos \xi \left( \sum_{\mu=1}^4 y_{\mu} y_{\mu} = 1 \right), \quad (33)$$

where  $\xi$  represents the azimuthal angle and  $y_m$  denote the coordinates of (normalized)  $S^3$  hyperlatitude:

$$\begin{aligned} y_1 &= \sin \chi \sin \theta \cos \phi, & y_2 &= \sin \chi \sin \theta \sin \phi, \\ y_3 &= \sin \chi \cos \theta, & y_4 &= \cos \chi. \end{aligned} \quad (34)$$

Normalized  $SO(5)$  monopole harmonics are represented as

$$\Psi_{N;j,m_j;k,m_k}(\xi, \chi, \theta, \phi) = G_{N,j,k}(\xi) \cdot \mathbf{Y}_{j,m_j;k,m_k}(\chi, \theta, \phi), \quad (35)$$

where

$$G_{N,j,k}(\xi) = (-1)^{2j+1} \sqrt{N + \frac{I}{2} + \frac{3}{2} \frac{1}{\sin \xi}} d_{N+\frac{I}{2}+1, -j+k, j+k+1}(\xi), \quad (36a)$$

$$\mathbf{Y}_{j,m_j;k,m_k}(\chi, \theta, \phi) = \sum_{m_R=-j}^j \begin{pmatrix} C_{j,m_R;\frac{I}{2},\frac{I}{2}}^{k,m_k} \Phi_{j,m_j;j,m_R}(\chi, \theta, \phi) \\ C_{j,m_R;\frac{I}{2},\frac{I}{2}-1}^{k,m_k} \Phi_{j,m_j;j,m_R}(\chi, \theta, \phi) \\ \vdots \\ C_{j,m_R;\frac{I}{2},-\frac{I}{2}}^{k,m_k} \Phi_{j,m_j;j,m_R}(\chi, \theta, \phi) \end{pmatrix}. \quad (36b)$$

Here,  $d_{l,m,m'}(\xi) \equiv \mathcal{D}_l(0, \xi, 0)_{m,m'}$  in (36a) stand for Wigner's small  $D$  matrices,  $C$ s in (36b) represent the Clebsch-Gordan coefficients, and  $\Phi$ s in (36b) denote the  $SO(4)$  spherical harmonics [54]. The  $SO(5)$  monopole harmonics satisfy

<sup>8</sup>In the original paper [81], they are referred to as the  $SU(2)$  monopole harmonics.

$$\int_{S^4} d\Omega_4 \Psi_{N;j,m_j;k,m_k}^\dagger \Psi_{N';j',m'_j;k',m'_k} = \delta_{N,N'} \delta_{j,j'} \delta_{k,k'} \delta_{m_j,m'_j} \delta_{m_k,m'_k} \quad (37)$$

and

$$\begin{aligned} \sum_{n=0}^N \sum_{s=-I/2}^{I/2} \sum_{m_j=-j}^j \sum_{m_k=-k}^k \Psi_{N;j,m_j;k,m_k} \Psi_{N;j,m_j;k,m_k}^\dagger \\ = \frac{(N+1)(I+N+2)(I+2N+3)}{16\pi^2} \mathbf{1}_{I+1}, \end{aligned} \quad (38)$$

where  $d\Omega_4 \equiv d\xi d\chi d\theta d\phi \sin^3 \xi \sin^2 \chi \sin \theta$ .

The  $SO(5)$  irreducible representation  $(p, q)_5 = (N + I, N)_5$  is decomposed as (see Fig. 3)

$$(N + I, N)_5 = \bigoplus_{n=0}^N (n) = \bigoplus_{n=0}^N \bigoplus_{s=-I/2}^{I/2} (j, k)_4, \quad (39)$$

where

$$(n) \equiv \bigoplus_{s=-I/2}^{I/2} (j, k)_4 \quad (40)$$

signifies the set of the  $SO(4)$  irreducible representations in the  $SO(4)$  line (the oblique line of the same color in Fig. 3). The  $N$ th  $SO(5)$  Landau level eigenstates consist of  $SO(4)$  irreducible representations on the  $SO(4)$  lines with  $n = 0, 1, 2, \dots, N$ . The  $SO(4)$  bispin index,  $(j, k)_4$ , is defined as

$$(j, k)_4 \equiv \left( \frac{n}{2} + \frac{I}{4} + \frac{s}{2}, \frac{n}{2} + \frac{I}{4} - \frac{s}{2} \right)_4, \quad (41)$$

with

$$n = 0, 1, 2, 3, \dots, N, \quad s = \frac{I}{2}, \frac{I}{2} - 1, \dots, -\frac{I}{2}. \quad (42)$$

The dimension of the  $SO(4)$  irreducible representation (41) is given by

$$\begin{aligned} d(n, I, s) &= (2j + 1)(2k + 1) \\ &= \left( n + \frac{I}{2} + s + 1 \right) \left( n + \frac{I}{2} - s + 1 \right) \\ &= d(n, I, -s), \end{aligned} \quad (43)$$

and that of the  $SO(4)$  line is

$$\begin{aligned} d(n, I) &\equiv \sum_{s=-I/2}^{I/2} d(n, I, s) \\ &= \frac{1}{6} (I + 1)(I^2 + (6n + 5)I + 6(n + 1)^2). \end{aligned} \quad (44)$$

Consequently, the  $N$ th Landau level degeneracy is counted as

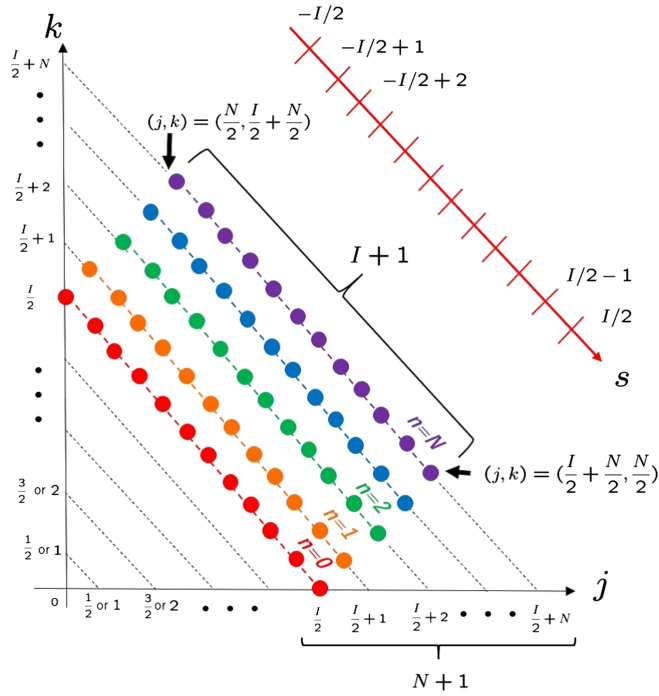


FIG. 3. Each of the filled circles represents an  $SO(4)$  irreducible representation  $(j, k)$ . The  $SO(4)$  irreducible representations denoted by the filled circles amount to the  $SO(5)$  irreducible representation  $(p, q)_5 = (N + I, N)_5$ . (Taken from [55].)

$$D(N, I) = \sum_{n=0}^N d(n, I) = \sum_{n=0}^N \sum_{s=-I/2}^{I/2} d(n, I, s) = \frac{1}{6}(N+1)(I+1)(I+N+2)(I+2N+3). \quad (45)$$

**B. Matrix coordinates**

The matrix coordinates have nonzero components only within the same Landau level and among adjacent Landau levels [55]:

$$\langle x_5 \rangle \neq 0 \rightarrow \Delta N = 0, \quad (46a)$$

$$\langle x_\mu \rangle \neq 0 \rightarrow \Delta N = 0, \pm 1. \quad (46b)$$

See the left of Fig. 4 where the nonzero matrix elements are denoted as the shaded color regions. Under the  $SO(4)$  rotation around the fifth axis,  $x_5$  behaves as a scalar  $(j, k) = (0, 0)$ , while  $x_\mu$  transform as a bispinor  $(j, k) = (1/2, 1/2)$ . From (41), we can see that the  $SO(4)$  selection rule implies that nonzero matrix coordinates exist only for

$$X_5^{[N]} \neq 0 \rightarrow (\Delta n, \Delta s) = (0, 0), \quad (47a)$$

$$X_\mu^{[N]} \neq 0 \rightarrow (\Delta n, \Delta s) = (\pm 1, 0), (0, \pm 1). \quad (47b)$$

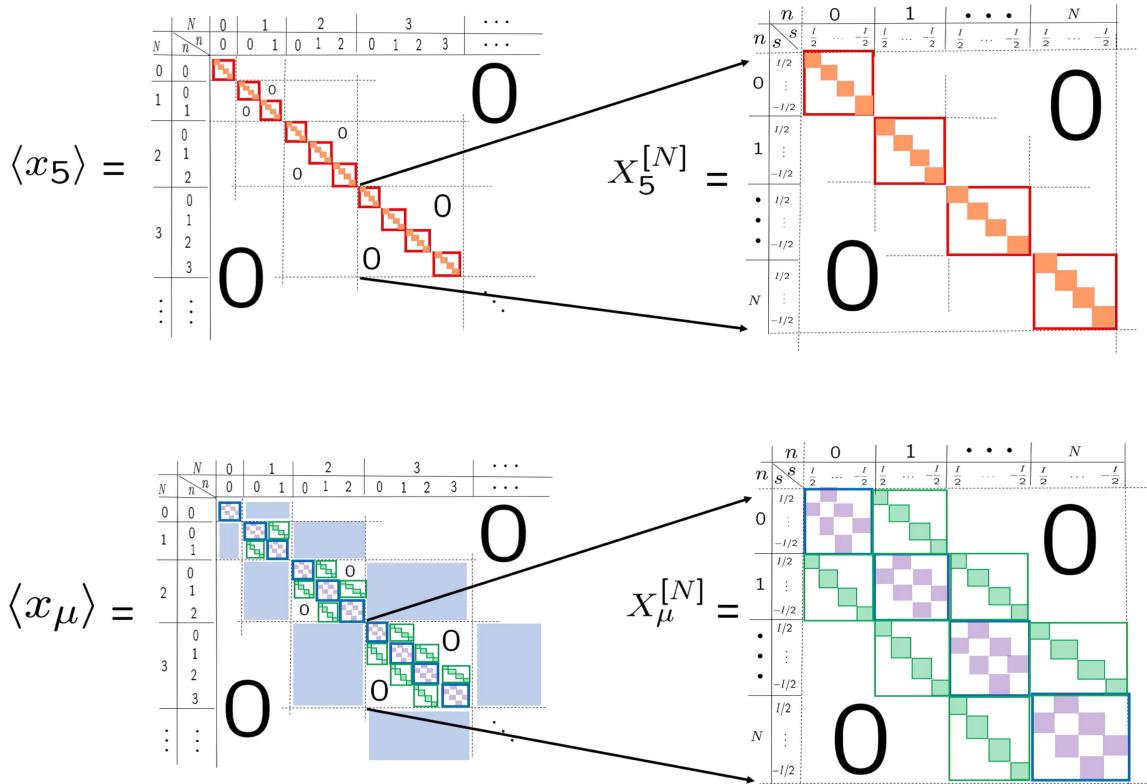


FIG. 4. The matrix coordinate representation of  $x_a$ .

Equations (47a)/(47b) correspond to the upper/lower right of Fig. 4. There are two cases in which  $X_\mu^{[N]}$  take finite values. The first is  $(\Delta n, \Delta s) = (\pm 1, 0)$  that corresponds to the green shaded rectangles in Fig. 4, representing transitions between two adjacent  $SO(4)$  lines in Fig. 3. The second  $(\Delta n, \Delta s) = (0, \pm 1)$  corresponds to the small purple shaded rectangles in Fig. 4, signifying transitions between two adjacent  $SO(4)$  irreducible representations on same  $SO(4)$  lines in Fig. 3. With this in mind, we will explicitly evaluate the matrix elements of  $x_a$ .

We can perform integrations of the azimuthal part and the  $S^3$  hyperlatitude part separately. For instance, the orthonormal condition (37) is evaluated as

$$\begin{aligned} & \langle \Psi_{N':j',m';k',m'_k} | \Psi_{N:j,m_j;k,m_k} \rangle \\ &= \langle G_{N',j',k'} | G_{N,j,k} \rangle \cdot \langle Y_{j',m';k',m'_k} | Y_{j,m_j;k,m_k} \rangle, \end{aligned} \quad (48)$$

where

$$\langle G_{N',j,k} | G_{N,j,k} \rangle = \int_0^\pi d\xi \sin^3 \xi G_{N,j,k}(\xi)^* G_{N',j,k}(\xi) = \delta_{N,N'}, \quad (49a)$$

$$\langle Y_{j',m';k',m'_k} | Y_{j,m_j;k,m_k} \rangle = \int_{S^3} d\chi d\theta d\phi \sin^2 \chi \sin \theta Y_{j,m_j;k,m_k}(\chi, \theta, \phi)^\dagger \times Y_{j',m';k',m'_k}(\chi, \theta, \phi) = \delta_{j,j'} \delta_{m_j,m'_j} \delta_{k,k'} \delta_{m_k,m'_k}. \quad (49b)$$

The matrix elements of  $X_5^{[N]}$  are derived as<sup>9</sup>

$$\begin{aligned} X_5^{[N]}: & -\langle \Psi_{N:j',m';k',m'_k} | x_5 | \Psi_{N:j,m_j;k,m_k} \rangle \\ &= -\langle G_{N,j,k} | x_5 | G_{N,j,k} \rangle \cdot \delta_{j,j'} \delta_{k,k'} \delta_{m_j,m'_j} \delta_{m_k,m'_k}, \end{aligned} \quad (50)$$

where

$$-\langle G_{N,j,k} | x_5 | G_{N,j,k} \rangle = \frac{2n+I+2}{(2N+I+2)(2N+I+4)} \cdot 2s. \quad (51)$$

The matrix coordinate (51) takes equally spaced discrete values specified by  $s = I/2, I/2 - 1, \dots, -I/2$ , which are regarded as the hyperlatitudes on fuzzy four-sphere. This structure is quite similar to that of the fuzzy two-sphere (Fig. 1). However notice that while the latitudes of fuzzy two-sphere are not degenerate, the hyperlatitudes of fuzzy four-sphere are degenerate, resulting in an intriguing internal structure as we shall discuss in Sec. V. Next, we turn to

$$X_\mu^{[N]}: \langle \Psi_{N:j',m';k',m'_k} | x_\mu | \Psi_{N:j,m_j;k,m_k} \rangle = \sum_{\sigma,\tau=\pm,-} \langle G_{N,j+\frac{\sigma}{2},k+\frac{\tau}{2}} | \sin \xi | G_{N,j,k} \rangle \langle Y_{j+\frac{\sigma}{2},m';k+\frac{\tau}{2},m'_k} | y_\mu | Y_{j,m_j;k,m_k} \rangle \delta_{j',j+\frac{\sigma}{2}} \delta_{k',k+\frac{\tau}{2}}. \quad (52)$$

Here, the azimuthal part is evaluated as

$$\langle G_{N,j+\frac{\sigma}{2},k+\frac{\tau}{2}} | \sin \xi | G_{N,j,k} \rangle = \delta_{\sigma,\tau} \langle G_{N,j+\frac{\sigma}{2},k+\frac{\tau}{2}} | \sin \xi | G_{N,j,k} \rangle + \delta_{\sigma,-\tau} \langle G_{N,j+\frac{\sigma}{2},k-\frac{\tau}{2}} | \sin \xi | G_{N,j,k} \rangle, \quad (53)$$

with<sup>10</sup>

$$\begin{aligned} \langle G_{N,j+\frac{\sigma}{2},k+\frac{\tau}{2}} | \sin \xi | G_{N,j,k} \rangle &= -\frac{4s}{(2N+I+2)(2N+I+4)} \sqrt{\left(N-n+\frac{1-\sigma}{2}\right) \left(N+n+I+2+\frac{1+\sigma}{2}\right)}, \\ \langle G_{N,j+\frac{\sigma}{2},k-\frac{\tau}{2}} | \sin \xi | G_{N,j,k} \rangle &= -\frac{4n+2I+4}{(2N+I+2)(2N+I+4)} \sqrt{\left(N+\frac{I}{2}-\sigma s+1\right) \left(N+\frac{I}{2}+\sigma s+2\right)}. \end{aligned} \quad (55)$$

<sup>9</sup>The minus sign in (50) is not essential but added for later convenience.

<sup>10</sup>In the derivation of (53), we used the formulas

$$\int_0^\pi d\theta \sin \theta d_{l,m',n}(\theta) \sin \theta d_{l,m,n}(\theta) |_{m'=m\pm 1} = \frac{2n}{(2l+1)(l+1)l} \sqrt{(l\pm m+1)(l\mp m)}, \quad (54a)$$

$$\int_0^\pi d\theta \sin \theta d_{l,m,n'}(\theta) \sin \theta d_{l,m,n}(\theta) |_{n'=n\pm 1} = -\frac{2m}{(2l+1)(l+1)l} \sqrt{(l\pm n+1)(l\mp n)}. \quad (54b)$$

The  $S^3$  hyperlatititude part is

$$\begin{aligned}
\langle Y_{j+\frac{\sigma}{2}, m'_j; k+\frac{\tau}{2}, m'_k} | y_1 | Y_{j, m_j; k, m_k} \rangle &= \frac{\sqrt{(2j+1)(2k+1)}}{2} (-1)^{n+I+\frac{\tau}{2}} \left\{ \begin{matrix} j+\frac{\sigma}{2} & k+\frac{\tau}{2} & \frac{1}{2} \\ k & j & \frac{1}{2} \end{matrix} \right\} \sum_{\kappa=+,-} (-1)^{\frac{\kappa-1}{2}} C_{\frac{1}{2}, \frac{\tau}{2}; j, m_j}^{j+\frac{\sigma}{2}, m'_j} C_{\frac{1}{2}, \frac{\tau}{2}; k, m_k}^{k+\frac{\tau}{2}, m'_k}, \\
\langle Y_{j+\frac{\sigma}{2}, m'_j; k+\frac{\tau}{2}, m'_k} | y_2 | Y_{j, m_j; k, m_k} \rangle &= -i \frac{\sqrt{(2j+1)(2k+1)}}{2} (-1)^{n+I+\frac{\tau}{2}} \left\{ \begin{matrix} j+\frac{\sigma}{2} & k+\frac{\tau}{2} & \frac{1}{2} \\ k & j & \frac{1}{2} \end{matrix} \right\} \sum_{\kappa=+,-} C_{\frac{1}{2}, \frac{\tau}{2}; j, m_j}^{j+\frac{\sigma}{2}, m'_j} C_{\frac{1}{2}, \frac{\tau}{2}; k, m_k}^{k+\frac{\tau}{2}, m'_k}, \\
\langle Y_{j+\frac{\sigma}{2}, m'_j; k+\frac{\tau}{2}, m'_k} | y_3 | Y_{j, m_j; k, m_k} \rangle &= -\frac{\sqrt{(2j+1)(2k+1)}}{2} (-1)^{n+I+\frac{\tau}{2}} \left\{ \begin{matrix} j+\frac{\sigma}{2} & k+\frac{\tau}{2} & \frac{1}{2} \\ k & j & \frac{1}{2} \end{matrix} \right\} \sum_{\kappa=+,-} C_{\frac{1}{2}, \frac{\tau}{2}; j, m_j}^{j+\frac{\sigma}{2}, m'_j} C_{\frac{1}{2}, -\frac{\tau}{2}; k, m_k}^{k+\frac{\tau}{2}, m'_k}, \\
\langle Y_{j+\frac{\sigma}{2}, m'_j; k+\frac{\tau}{2}, m'_k} | y_4 | Y_{j, m_j; k, m_k} \rangle &= i \frac{\sqrt{(2j+1)(2k+1)}}{2} (-1)^{n+I+\frac{\tau}{2}} \left\{ \begin{matrix} j+\frac{\sigma}{2} & k+\frac{\tau}{2} & \frac{1}{2} \\ k & j & \frac{1}{2} \end{matrix} \right\} \sum_{\kappa=+,-} (-1)^{\frac{\kappa-1}{2}} C_{\frac{1}{2}, \frac{\tau}{2}; j, m_j}^{j+\frac{\sigma}{2}, m'_j} C_{\frac{1}{2}, -\frac{\tau}{2}; k, m_k}^{k+\frac{\tau}{2}, m'_k}, \quad (56)
\end{aligned}$$

where  $C_{\frac{1}{2}, \frac{\tau}{2}; j, m}^{j+\frac{\sigma}{2}, m'}$  denote the Clebsch-Gordan coefficients:

$$C_{\frac{1}{2}, \frac{\tau}{2}; j, m}^{j+\frac{\sigma}{2}, m'} = \delta_{m', m+\frac{\tau}{2}} \left( \delta_{\tau, 1} \sqrt{\frac{j+\kappa m+1}{2j+1}} + \kappa \delta_{\tau, -1} \sqrt{\frac{j+\kappa m}{2j+1}} \right). \quad (57)$$

The formulas of Appendix D in [55] were utilized in the derivation of Eq. (56). We thus derived the explicit form of the matrix coordinates in the  $SO(5)$  Landau levels. For a better understanding, in Appendix C of Ref. [82], we provide the matrix coordinates for the case of  $(N, I) = (1, 1)$ . Note that all of the quantities involved in the matrix coordinate calculations, such as an integral measure and  $S^4$  coordinates, are  $SO(5)$  invariant or covariant quantities. Consequently, the obtained matrix coordinates are necessarily  $SO(5)$  covariant coordinates that transform as the  $SO(5)$  vector like the original  $S^4$  coordinates [see Eq. (86)].

In the case of  $I = 0$ , the gauge symmetry no longer exists. Therefore, we cannot expect fuzzy geometries (recall that the gauge symmetry is crucial in the present scheme). Indeed, when  $I = 0$ , the energy eigenstates are given by the  $SO(5)$  spherical harmonics and the matrix coordinates become trivial:

$$X_a^{[N]} = 0. \quad (58)$$

The corresponding dimensions of the  $SO(5)$  spherical harmonics are

$$D(N, I=0) = \frac{1}{6}(N+1)(N+2)(2N+3) = 5, 14, 30, \dots \quad (59)$$

Therefore in these matrix dimensions, the matrix geometries do not exist. In Ref. [16], the authors argued the nonexistence of five-dimensional matrix coordinates, which corresponds to the smallest dimension in Eq. (59).

#### IV. PURE QUANTUM NAMBU MATRIX GEOMETRY

Using the explicit matrix coordinates, we now expand concrete discussions about the matrix geometries. It is shown that the matrix coordinates satisfy

$$\sum_{a=1}^5 X_a^{[N]} X_a^{[N]} = c_1(N, I) \mathbf{1} \quad (60)$$

and

$$[X_a^{[N]}, X_b^{[N]}, X_c^{[N]}, X_d^{[N]}] = 4! c_3(N, I) \sum_{e=1}^5 \epsilon_{abcde} X_e^{[N]}, \quad (61)$$

where the quantum Nambu bracket denotes the totally antisymmetric combination of the four quantities inside the bracket:

$$[O_1, O_2, O_3, O_4] \equiv \text{sgn}(\sigma) O_{\sigma_1} O_{\sigma_2} O_{\sigma_3} O_{\sigma_4}. \quad (62)$$

(Detail discussions about the coefficients,  $c_1$  and  $c_3$ , will be given in Sec. IV B.) Equations (60) and (61) signify a realization of the fuzzy four-sphere [15,16]. The quantum Nambu geometry thus emerges as the matrix geometry in the  $SO(5)$  Landau levels. We delve into geometric structures hidden in the mathematics of the quantum Nambu algebra using the explicit form of the matrix coordinates.

##### A. The lowest Landau level matrix geometry

For  $N = 0$ , Eqs. (50) and (52) reproduce the lowest Landau level matrix coordinates previously obtained in [55,60]:

$$X_a^{[0]} = \frac{1}{I+4} \Gamma_a, \quad (63)$$

where  $\Gamma^a$  represents the  $I$ -fold symmetric tensor product of the  $SO(5)$  gamma matrices [16]:

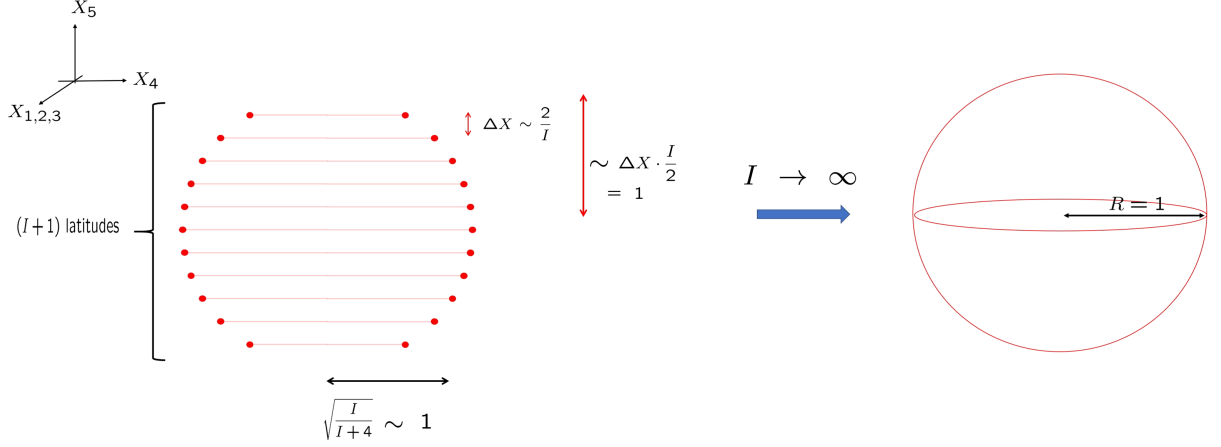


FIG. 5. Fuzzy four-sphere in the lowest Landau level (the left) and its continuum limit (the right).

$$\Gamma^a = (\gamma^a \otimes 1 \otimes \cdots \otimes 1 + 1 \otimes \gamma^a \otimes \cdots \otimes 1 + \cdots + 1 \otimes 1 \otimes \cdots \otimes \gamma_a)_{\text{sym}} \quad (64)$$

with

$$\gamma_i = \begin{pmatrix} 0 & i\sigma_i \\ -i\sigma_i & 0 \end{pmatrix}, \quad \gamma_4 = \begin{pmatrix} 0 & 1_2 \\ 1_2 & 0 \end{pmatrix}, \quad \gamma_5 = \begin{pmatrix} 1_2 & 0 \\ 0 & -1_2 \end{pmatrix}. \quad (65)$$

We can readily check that  $X_a^{[0]}$  satisfy (60) and (61),

$$\sum_{a=1}^5 X_a^{[0]} X_a^{[0]} = \frac{I}{I+4} \mathbf{1}_{\frac{1}{6}(I+1)(I+2)(I+3)} \quad (66)$$

and

$$[X_a^{[0]}, X_b^{[0]}, X_c^{[0]}, X_d^{[0]}] = -(I+2) \left( \frac{2}{I+4} \right)^3 \epsilon_{abcde} X_e^{[0]}. \quad (67)$$

The radius and the noncommutative scale are derived as

$$R = \sqrt{\frac{I}{I+4}} \quad (I \rightarrow \infty \rightarrow 1),$$

$$\Delta X = \frac{2}{I+4} \quad (I \rightarrow \infty \rightarrow 0), \quad (68)$$

which implies that the ordinary four-sphere with a unit radius is reproduced in the continuum limit (Fig. 5).

It should be emphasized that the algebra of  $X_a$  can be described within the commutator formalism, and the quantum Nambu algebra (67) is not indispensable for the description of the lowest Landau level matrix geometry. The matrix coordinates  $X_a^{[0]}$  and  $X_{ab}^{[0]} \equiv -i\frac{1}{4}[X_a^{[0]}, X_b^{[0]}]$  satisfy a closed algebra

$$[X_a^{[0]}, X_b^{[0]}] = 4i \frac{1}{(I+4)^2} X_{a,b}^{[0]},$$

$$[X_a^{[0]}, X_{bc}^{[0]}] = -i\delta_{ab} X_c^{[0]} + i\delta_{ac} X_b^{[0]},$$

$$[X_{ab}^{[0]}, X_{cd}^{[0]}] = i\delta_{ac} X_{bd}^{[0]} - i\delta_{ad} X_{bc}^{[0]} + i\delta_{bd} X_{ac}^{[0]} - i\delta_{bc} X_{ad}^{[0]}, \quad (69)$$

which is the  $SU(4)$  [20]. The quantum Nambu algebra (67) is not exactly equivalent with the  $SU(4)$  algebra (69); however, they have been treated almost synonymously thus far. This is because the known matrix realization of the fuzzy four-sphere was only the fully symmetric representation that satisfies both (67) and (69). The closed algebra (69) suggests that the natural symmetry in the lowest Landau level is the  $SU(4)$  rather than the original  $SO(5)$ . This becomes clearer in the following discussion. The symmetric representation can be simply realized using the Schwinger boson operators<sup>11</sup>:

$$X_a^{[0]} = \frac{1}{I+4} \hat{\psi}_\alpha^\dagger (\gamma_a)_{\alpha\beta} \hat{\psi}_\beta \quad (70)$$

with

$$[\hat{\psi}_\alpha, \hat{\psi}_\beta^\dagger] = \delta_{\alpha\beta}, \quad [\hat{\psi}_\alpha, \hat{\psi}_\beta] = 0. \quad (71)$$

The boson number indicates the  $SU(2)$  index of Yang's monopole:

$$\sum_{\alpha=1}^4 \hat{\psi}_\alpha^\dagger \hat{\psi}_\alpha = I. \quad (72)$$

One may readily check that (70) satisfy the  $SU(4)$  algebra (69) together with  $X_{ab}^{[0]} = -i\frac{1}{4}\hat{\psi}_\alpha^\dagger([\gamma_a, \gamma_b])_{\alpha\beta}\hat{\psi}_\beta$ . The fuzzy

<sup>11</sup>Historically, the Schwinger boson operators were utilized in the first construction of the fuzzy four-sphere [15].

manifold constructed from the  $SU(4)$  matrices of the  $SU(4)$  fully symmetric representation is referred to as the fuzzy  $\mathbb{C}P^3$  [19]. Note that the dimension of the  $SO(5)$  lowest Landau level  $(p, q)_5 = (I, 0)_5$ , is exactly equal to that of the  $SU(4)$  fully symmetric representation:

$$D(0, I) = \frac{1}{3!} (I+1)(I+2)(I+3). \quad (73)$$

Therefore, the fuzzy  $S^4$  is equivalent to the fuzzy  $\mathbb{C}P^3$  (see Ref. [83] for discussions including matrix functions on them). The commutation relations of the Schwinger boson operators correspond to the canonical quantization of the homogeneous coordinates of the symplectic manifold  $\mathbb{C}P^3$ . Therefore, it may be reasonable that the lowest Landau level geometry can be described within the conventional commutator formalism of the Lie algebra. The corresponding continuum limit is  $\mathbb{C}P^3$ , which is the coset

$$\mathbb{C}P^3 \simeq SU(4)/U(3). \quad (74)$$

Here, we encounter the  $SU(4)$  symmetry again. It is also worth noting that  $\mathbb{C}P^3$  is locally equivalent to

$$\mathbb{C}P^3 \sim S^4 \times S^2. \quad (75)$$

While the original  $S^4$  itself is not a symplectic manifold, the  $S^2$ -fiber twisted on  $S^4$  makes the entire bundle symplectic.

### B. Higher Landau level matrix geometry

From (50), we have

$$\begin{aligned} \text{tr}(X_5^{[N]^2}) &= \frac{1}{(2N+I+4)^2(2N+I+2)^2} \sum_{n=0}^N (I+2+2n)^2 \\ &\times \sum_{s=-I/2}^{I/2} (2s)^2 d(n, I, s) \\ &= \frac{1}{5} c_1(N, I) D(N, I), \end{aligned} \quad (76)$$

where

$$c_1(N, I) \equiv \frac{I(I+2)}{(2N+I+4)(2N+I+2)}. \quad (77)$$

Since all of  $X_a^{[N]}$  are related by unitary transformations, their traces are the same,  $\text{tr}(X_1^{[N]^2}) = \text{tr}(X_2^{[N]^2}) = \dots = \text{tr}(X_5^{[N]^2}) = \frac{1}{5} c_1 D$ . The orthonormal relation for  $X_a[N]$  is given by

$$\text{tr}(X_a^{[N]} X_b^{[N]}) = \frac{1}{5} c_1(N, I) D(N, I) \delta_{ab}, \quad (78)$$

which implies Eq. (60):

$$\sum_{a=1}^5 X_a^{[N]} X_a^{[N]} = c_1(N, I) \mathbf{1}_{D(N, I)}. \quad (79)$$

One can explicitly check the validity of Eq. (79) using Eqs. (50) and (52). The radius of the fuzzy four-sphere is given by

$$\begin{aligned} R(N, I) &\equiv \sqrt{c_1(N, I)} \\ &= \sqrt{\frac{I(I+2)}{(2N+I+4)(2N+I+2)}} \sim \frac{I}{2N+I}. \end{aligned} \quad (80)$$

Since the matrix coordinates have two parameters,  $N$  and  $I$ , there are two different infinity limits of the radius:

$$\lim_{I \rightarrow \infty} R(N, I) = 1, \quad (81a)$$

$$\lim_{N \rightarrow \infty} R(N, I) = 0. \quad (81b)$$

Equation (81a) signifies the usual commutative limit in which the fuzzy four-sphere is reduced to the continuum four-sphere with a unit radius. On the other hand, Eq. (81b) indicates the collapse of the fuzzy four-spheres at  $N \rightarrow \infty$ . We will revisit this in Sec. IV C. It is demonstrated that  $X_a^{[N]}$  satisfy the quantum Nambu algebra (61):

$$[X_a^{[N]}, X_b^{[N]}, X_c^{[N]}, X_d^{[N]}] = -4! c_3(N, I) \epsilon_{abcde} X_e^{[N]}, \quad (82)$$

where

$$c_3(N, I) \equiv -\frac{5}{c_1(N, I) D(N, I)} \text{tr}(X_1^{[N]} X_2^{[N]} X_3^{[N]} X_4^{[N]} X_5^{[N]}). \quad (83)$$

For instance,  $\text{tr}(X_1^{[N]} X_2^{[N]} X_3^{[N]} X_4^{[N]} X_5^{[N]}) = -\frac{2896}{7503125} - \frac{217}{124416} - \frac{856}{5250987}$  for  $(N, I) = (1, 1), (1, 2), (2, 1)$ .<sup>12</sup> The matrix coordinates of the higher Landau levels not only satisfy the quantum Nambu algebra (82) but also encompass all possible matrix realizations of that algebra, because the higher Landau level matrix geometries encompass all possible irreducible representations of  $SO(5)$ .

<sup>12</sup>In the lowest Landau level, we have

$$\begin{aligned} \text{tr}(X_1^{[0]} X_2^{[0]} X_3^{[0]} X_4^{[0]} X_5^{[0]}) &= \left(\frac{1}{I+4}\right)^5 \text{tr}(\Gamma_1 \Gamma_2 \Gamma_3 \Gamma_4 \Gamma_5) \\ &= -\frac{1}{90(I+4)^4} I(I+1)(I+2)^2(I+3), \end{aligned} \quad (84)$$

and Eq. (82) reproduces Eq. (67).

It is also easy to see

$$[X_a^{[N]}, X_b^{[N]}] \propto i\Sigma_{ab}^{[N]} \quad (N \geq 1), \quad (85)$$

where  $\Sigma_{ab}^{[N]}$  denote the  $SO(5)$  generators in the  $(N+I, I)_5$  representation. Equation (85) is consistent with the general discussions in Sec. II C 2. While the commutators of  $X_a$  do not give rise to the  $SO(5)$  generators,  $X_a$  themselves transform as an  $SO(5)$  vector:

$$[X_a^{[N]}, \Sigma_{bc}^{[N]}] = -i\delta_{ab}X_c^{[N]} + i\delta_{ac}X_b^{[N]}. \quad (86)$$

The higher Landau level geometry is thus the one that adheres to the quantum Nambu algebra but not the  $SU(4)$  algebra in contrast to the lowest Landau level matrix geometry. Let us recall again that the present scheme is beyond the conventional commutator formalism. The quantum geometry in the higher Landau levels is thus qualitatively different to that of the lowest Landau level. The algebraic structure of the higher Landau level geometry

is apparent only after introducing the quantum Nambu bracket and cannot be captured by the ordinary commutator formalism. In this sense, the higher Landau level geometry is considered to be a pure quantum Nambu geometry.

### C. Nested fuzzy four-sphere

Let us delve into the matrix structure of  $X_a^{[N]}$ . We represent (50) by the following  $D(N, I) \times D(N, I)$  matrix (the upper left of Fig. 6):

$$X_5^{[N]} = \bigoplus_{n=0}^N X_5^{(n)} = \begin{pmatrix} X_5^{(0)} & 0 & 0 & 0 & 0 \\ 0 & X_5^{(1)} & 0 & 0 & 0 \\ 0 & 0 & X_5^{(2)} & 0 & 0 \\ 0 & 0 & 0 & \ddots & 0 \\ 0 & 0 & 0 & 0 & X_5^{(N)} \end{pmatrix}, \quad (87)$$

where

$$X_5^{(n)} = \frac{I+2n+2}{(2N+I+4)(2N+I+2)} \bigoplus_{s=-I/2}^{I/2} 2s \mathbf{1}_{d(n, I, s)},$$

$$= \frac{I+2n+2}{(2N+I+4)(2N+I+2)} \begin{pmatrix} I\mathbf{1}_{d(n, I, I/2)} & 0 & 0 & 0 & 0 \\ 0 & (I-2)\mathbf{1}_{d(n, I, I/2-1)} & 0 & 0 & 0 \\ 0 & 0 & (I-4)\mathbf{1}_{d(n, I, I/2-2)} & 0 & 0 \\ 0 & 0 & 0 & \ddots & 0 \\ 0 & 0 & 0 & 0 & -I\mathbf{1}_{d(n, I, -I/2)} \end{pmatrix}. \quad (88)$$

The diagonal blocks in  $X_\mu^{[N]}$  that correspond to  $X_5^{(n)}$  are denoted as  $X_\mu^{(n)}$  (the lower right in Fig. 6), which signify the matrix coordinates on the  $SO(4)$  line ( $n$ ). We will delve into the matrix structure of  $X_a^{(n)}$  that represents the fuzzy geometry on the  $SO(4)$  line ( $n$ ). The sum of the squares of  $X_a^{(n)}$  is given by

$$\sum_{a=1}^5 X_a^{(n)} X_a^{(n)} = \bigoplus_{s=-I/2}^{I/2} R^{(n, s)^2} \mathbf{1}_{d(n, I, s)} = \begin{pmatrix} R^{(n, I/2)^2} \mathbf{1}_{(n+I+1)(n+1)} & 0 & \dots & 0 \\ 0 & R^{(n, I/2-1)^2} \mathbf{1}_{(n+I)(n+2)} & 0 & 0 \\ \vdots & 0 & \ddots & 0 \\ 0 & 0 & 0 & R^{(n, -I/2)^2} \mathbf{1}_{(n+1)(n+I+1)} \end{pmatrix}, \quad (89)$$

where

$$R^{(n, s)} \equiv \frac{I+2n+2}{(2N+I+4)(2N+I+2)} \sqrt{2(B(j, k) + B(k, j)) + (2s)^2} = R^{(n, -s)} \quad (90)$$

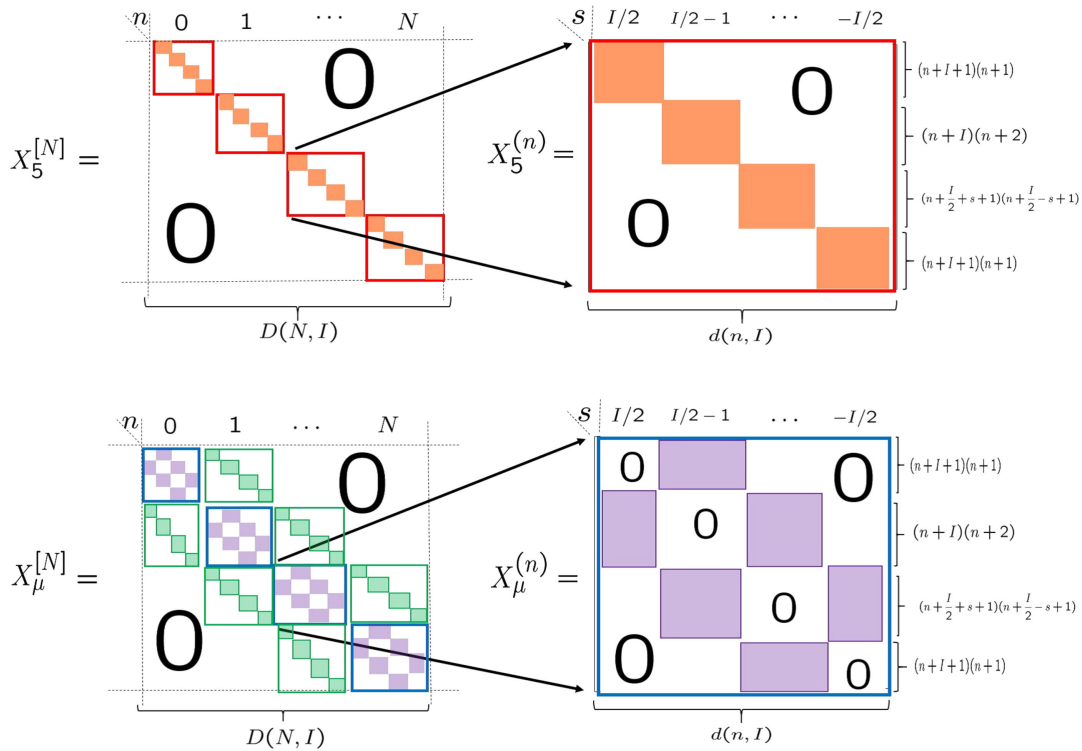


FIG. 6. Matrix coordinates of the  $N$ th Landau level. Nonzero matrix elements are denoted as the shaded color regions.

with  $B(j, k)$  defined by (104). Thus,  $\sum_{a=1}^5 X_a^{(n)} X_a^{(n)}$  is not proportional to unit matrix  $\mathbf{1}_{d(n, I)}$  (except for the special case  $I = 1$ ),<sup>13</sup> and so  $X_a^{(n)}$  does not give rise to a complete fuzzy four-sphere geometry but provides a fuzzy four-sphere-like structure referred to as the quasifuzzy four-sphere [55]. The  $I + 1$  diagonal blocks on the most right-hand side of Eq. (89) signify the  $I + 1$  fuzzy hyperlatitudes on the quasifuzzy four-sphere. Inside the matrix coordinates  $X_a^{[N]}$  (Fig. 6), there exist such  $N + 1$  quasifuzzy four-spheres  $X_a^{(n=0,1,2,\dots,N)}$ . The nonzero off-diagonal blocks of the  $X_\mu^{[N]}$  (the green filled rectangles in the lower left of Fig. 6) are interpreted as the interactions between the adjacent quasifuzzy four-spheres.

The nested geometry of the  $N + 1$  quasifuzzy four-spheres is depicted in Fig. 7. One should not confuse the present geometry with the nested structure made of a completely reducible representation [84]: In the case of

<sup>13</sup>For  $I = 1$ , we have only two hyperlatitudes with the same radius, and  $\sum_{a=1}^5 X_a^{(n)} X_a^{(n)}$  is proportional to  $\mathbf{1}$ :

$$\sum_{\mu=1}^a X_a^{(n)} X_a^{(n)} = \left( \frac{2n+3}{(2N+5)(2N+3)} \right)^2 \left( 2 \frac{(N+2)^2}{(n+2)(n+1)} + 1 \right) \times \mathbf{1}_{2d(n,1)=2(n+2)(n+1)}. \quad (91)$$

the completely reducible representation, the nested fuzzy structure originates from the direct sum of the irreducible representations, while in the present, the nested fuzzy four-sphere is constituted from a single  $SO(5)$  irreducible representation and each of the quasifuzzy four-spheres is not made of an  $SO(5)$  irreducible representation [but rather consists of the  $SO(4)$  representations on the  $SO(4)$  line].<sup>14</sup> Consequently, each quasifuzzy four-sphere is not regarded as an  $SO(5)$ -symmetric object. This is also evident from the right-hand side of (89), which is apparently not  $SO(5)$  invariant. The quasifuzzy four-spheres along with their interactions collectively form an  $SO(5)$ -symmetric fuzzy manifold. We would like to draw the analogy to benzene. Each Kekulé structure only respects the  $C_3$  rotational symmetry, while quantum mechanical superposition of two Kekulé structures results in benzene, which exhibits higher  $C_6$  symmetry. Such a structure cannot be comprehended without quantum mechanics, and benzene realizes a purely quantum mechanical structure with no classical counterpart. In a similar sense, the nested fuzzy four-sphere can be considered a pure quantum geometry. This stems from the present quantum-oriented scheme, which can encompass pure quantum geometries.

<sup>14</sup>The very fuzzy fibers of fuzzy geometry is reported in [85–87]. That structure originates from the direct sum of irreducible representations, and so it is more akin to [84] than the present one.

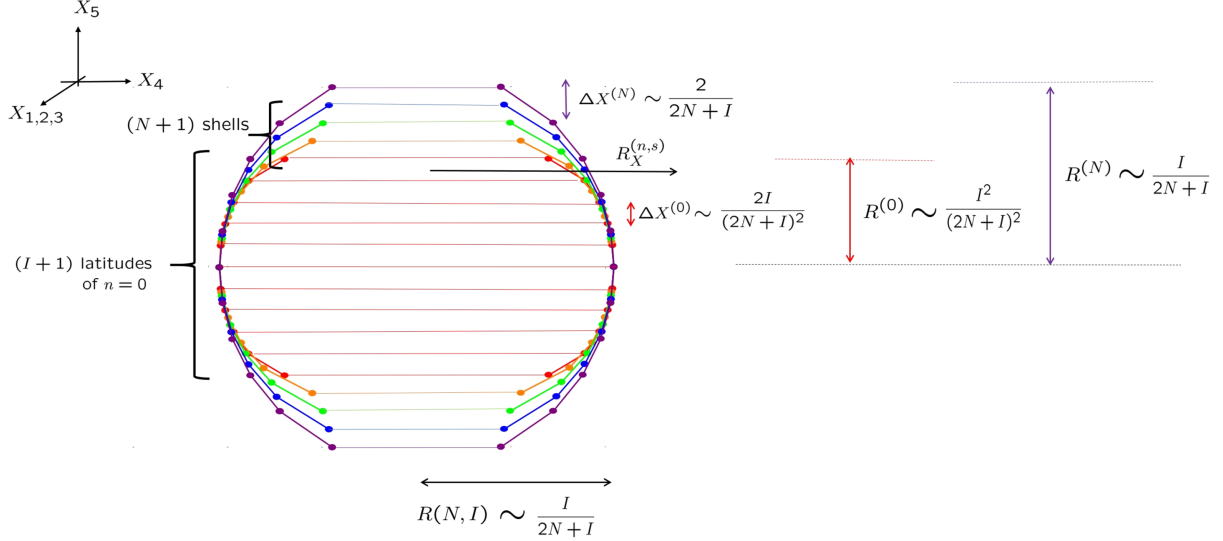


FIG. 7. Matrix geometry of the  $N$ th higher Landau level is constituted from the  $N + 1$  quasifuzzy four-spheres (and their interactions) to exhibit a nested fuzzy structure.

The noncommutative scale differs in each of the quasifuzzy four-spheres (88):

$$\Delta X^{(n)} = \frac{2}{(2N + I + 4)(2N + I + 2)} (2n + I + 2), \quad (92)$$

and the “radius” of the quasifuzzy four-sphere is estimated as

$$R^{(n)} \sim \Delta X^{(n)} \cdot \frac{I}{2} = \frac{1}{(2N + I + 4)(2N + I + 2)} (2n + I + 2)(I + 1) \sim \frac{(2n + I)I}{(2N + I)^2}. \quad (93)$$

The outer quasifuzzy four-spheres have wider noncommutative scales (see Fig. 7). It can be confirmed that the outermost quasifuzzy four-sphere of  $n = N$  (93) exhibits the same behavior as the nested fuzzy four-sphere (80), as anticipated. We now provide an intuitive explanation for the previous result of the two limits (81). In the commutative limit  $I \rightarrow \infty$ , while  $\Delta X^{(n)} \sim \frac{2}{I}$  (92) is reduced to zero, the number of the hyperlatitudes  $I$  goes to infinity. These two contributions are compensated to realize a continuum four-sphere with a unit radius, which simultaneously implies that all of the  $N + 1$  quasifuzzy four-spheres are reduced to the single four-sphere.<sup>15</sup> On the other hand, in the limit  $N \rightarrow \infty$ , while the number of hyperlatitudes remains

<sup>15</sup>In the commutative limit  $I \rightarrow \infty$ , each point on the four-sphere is highly degenerate. Because of the  $SO(5)$  symmetry, we can count this degeneracy, for instance, at the north pole  $X_5^{(n)} = 1$ :

$$I \sum_{n=0}^N (n + 1) = I \frac{1}{2} (N + 1)(N + 2). \quad (94)$$

unchanged, the noncommutative length (92)  $\Delta X^{(n)} \sim \frac{1}{N}$  converges to zero. This leads to the collapse of the very nested fuzzy four-sphere,  $R^{(n)} \rightarrow 0$  (Fig. 8).

## V. INTERNAL MATRIX GEOMETRY

Fuzzy three-sphere geometry can be realized as a submanifold of the (unnested) fuzzy four-sphere. Here, we explore the generalization of this concept for the nested fuzzy four-spheres.

### A. Fuzzy hyperlatitudes

The quasifuzzy four-sphere is constituted from the  $SO(4)$  irreducible representations on the  $SO(4)$  line ( $n$ ). The matrix coordinates of the hyperlatitudes on the quasifuzzy four-sphere are readily derived from Eq. (56):

$$(Y_\mu^{(n)})_{m'_j, m'_k; m_j, m_k} \equiv \langle Y_{j', m'_j, k', m'_k} | Y_\mu | Y_{j, m_j, k, m_k} \rangle \Big|_{j'+k'=j+k=n+\frac{1}{2}}, \quad (95)$$

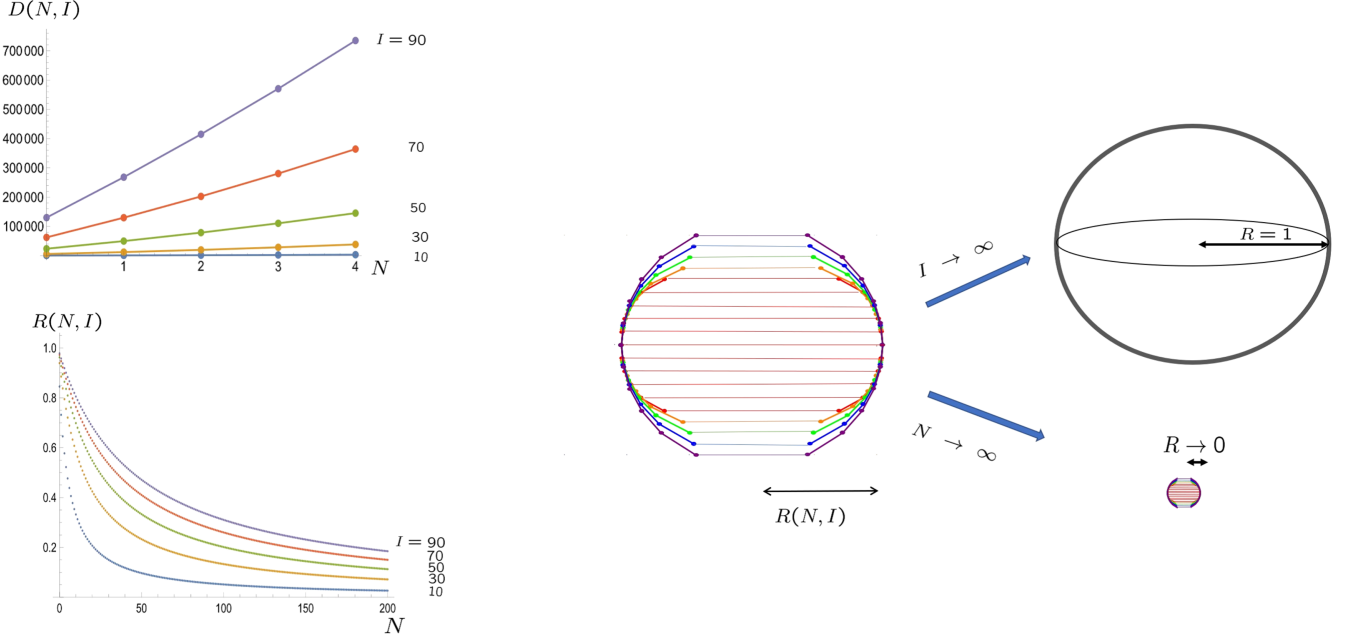


FIG. 8. Behaviors of the quantities of the nested fuzzy four-sphere: The degeneracies (the upper left) and the radii (the lower left), the continuum limit  $I \rightarrow \infty$  (the upper right) and the  $N \rightarrow \infty$  limit (the lower right).

which denotes a  $d(n, I) \times d(n, I)$  matrix.<sup>16</sup> The sum of the squares of  $Y_\mu^{(n)}$  is given by

$$\sum_{\mu=1}^4 Y_\mu^{(n)} Y_\mu^{(n)} = \bigoplus_{s=-I/2}^{I/2} \mathcal{R}_Y^{(n,s)2} \mathbf{1}_{d(n,I,s)} = \begin{pmatrix} \mathcal{R}_Y^{(n, \frac{I}{2})2} \mathbf{1}_{(n+I+1)(n+1)} & 0 & \cdots & 0 \\ 0 & \mathcal{R}_Y^{(n, \frac{I}{2}-1)2} \mathbf{1}_{(n+I)(n+2)} & 0 & 0 \\ 0 & 0 & \ddots & 0 \\ 0 & 0 & 0 & \mathcal{R}_Y^{(n, -\frac{I}{2})2} \mathbf{1}_{(n+I+1)(n+1)} \end{pmatrix}, \quad (98)$$

<sup>16</sup>The matrix  $Y_\mu^{(n)}$  has the same matrix form as  $X_\mu^{(n)}$  (the lower right of Fig. 6):

$$Y_\mu^{(n)} = \begin{pmatrix} 0 & \mathcal{Y}_\mu^{(+)} \left( \frac{I+n-1}{2}, \frac{n+1}{2} \right) & 0 & 0 & 0 & 0 \\ \mathcal{Y}_\mu^{(+)} \left( \frac{I+n-1}{2}, \frac{n+1}{2} \right)^\dagger & 0 & \mathcal{Y}_\mu^{(+)} \left( \frac{I+n-2}{2}, \frac{n+2}{2} \right) & 0 & 0 & 0 \\ 0 & \mathcal{Y}_\mu^{(+)} \left( \frac{I+n-2}{2}, \frac{n+2}{2} \right)^\dagger & 0 & \mathcal{Y}_\mu^{(+)} \left( \frac{I+n-3}{2}, \frac{n+3}{2} \right) & 0 & 0 \\ 0 & 0 & \mathcal{Y}_\mu^{(+)} \left( \frac{I+n-3}{2}, \frac{n+3}{2} \right)^\dagger & 0 & \ddots & 0 \\ 0 & 0 & 0 & \ddots & 0 & \mathcal{Y}_\mu^{(+)} \left( \frac{n}{2}, \frac{n+I}{2} \right) \\ 0 & 0 & 0 & 0 & \mathcal{Y}_\mu^{(+)} \left( \frac{n}{2}, \frac{n+I}{2} \right)^\dagger & 0 \end{pmatrix}, \quad (96)$$

and  $A(j, k)$  and  $A(k, j)$  in (99) are given by

$$\sum_{\mu=1}^4 \mathcal{Y}_\mu^{(+)}(j, k)^\dagger \mathcal{Y}_\mu^{(+)}(j, k) = A(j, k) \mathbf{1}_{(2j+1)(2k+1)}, \quad (97a)$$

$$\sum_{\mu=1}^4 \mathcal{Y}_\mu^{(+)} \left( j - \frac{1}{2}, k + \frac{1}{2} \right) \mathcal{Y}_\mu^{(+)} \left( j - \frac{1}{2}, k + \frac{1}{2} \right)^\dagger = A(k, j) \mathbf{1}_{(2j+1)(2k+1)}. \quad (97b)$$

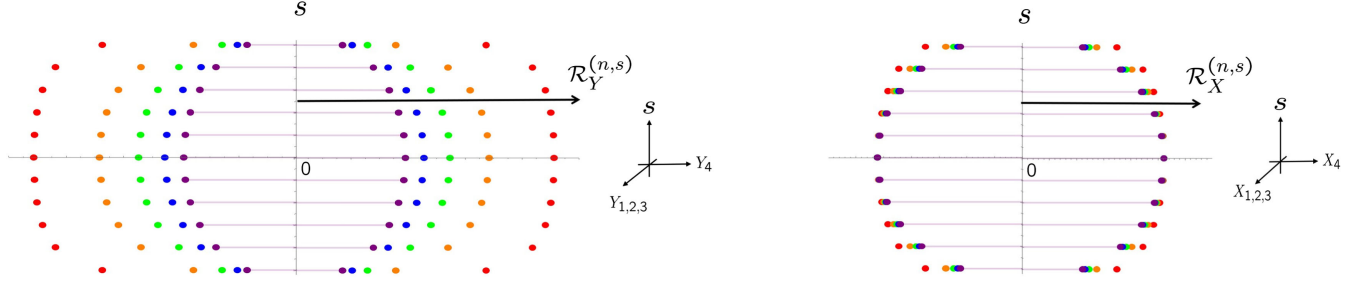


FIG. 9. The distributions of  $\mathcal{R}_Y^{(n,s)}$  (the left) and  $\mathcal{R}_X^{(n,s)}$  (the right) for  $I/2 = 5$ . The  $SO(4)$  line index  $n(= 0, 1, 2, 3, 4)$  corresponds to red, orange, green, blue, and purple points, respectively.

where

$$\mathcal{R}_Y^{(n,s)} \equiv \sqrt{A(j,k) + A(k,j)} = \mathcal{R}_Y^{(n,-s)} \quad (99)$$

with

$$A(j,k) \equiv 2(j+1)k \begin{Bmatrix} j + \frac{1}{2} & k - \frac{1}{2} & \frac{I}{2} \\ k & j & \frac{1}{2} \end{Bmatrix}^2. \quad (100)$$

Note that  $A(\frac{n}{2} + \frac{I}{2}, \frac{n}{2}) = 0$ . Equation (98) represents a block diagonal matrix, with diagonal blocks indicating the hyper

latitudes of the radius  $\mathcal{R}_Y^{(n,s)}$ . At  $I \rightarrow \infty$  and  $|s| \ll I$ , we have

$$\mathcal{R}_Y^{(n,s)} \rightarrow 1 \quad \left( A(j,k) \rightarrow \frac{1}{2} \right). \quad (101)$$

Around  $s \sim 0$ , the radii of the hyperlatitudes converge to unity, as anticipated from  $\sum_{\mu=1}^4 y_\mu y_\mu = 1$ . The hyperlatitudes for  $s$  as the vertical axis are depicted in the left of Fig. 9.

We also evaluate the radii of the hyperlatitudes within the quasifuzzy four-sphere. Using Eq. (52), we can derive

$$\sum_{\mu=1}^4 X_\mu^{(n)} X_\mu^{(n)} = \bigoplus_{s=-I/2}^{I/2} \mathcal{R}_X^{(n,s)2} \mathbf{1}_{d(n,I,s)} = \begin{pmatrix} \mathcal{R}_X^{(n, \frac{I}{2})2} \mathbf{1}_{(n+I+1)(n+1)} & 0 & \cdots & 0 \\ 0 & \mathcal{R}_X^{(n, \frac{I}{2}-1)2} \mathbf{1}_{(n+I)(n+2)} & 0 & 0 \\ 0 & 0 & \ddots & 0 \\ 0 & 0 & 0 & \mathcal{R}_X^{(n, -\frac{I}{2})2} \mathbf{1}_{(n+I+1)(n+1)} \end{pmatrix}, \quad (102)$$

where

$$\begin{aligned} \mathcal{R}_X^{(n,s)} &\equiv \frac{2n + I + 2}{(2N + I + 2)(2N + I + 4)} \sqrt{B(j,k) + B(k,j)} \\ &= \mathcal{R}_X^{(n,-s)}, \end{aligned} \quad (103)$$

with

$$\begin{aligned} B(j,k) &\equiv 4 \left( N + \frac{I}{2} - j + k + 1 \right) \\ &\quad \times \left( N + \frac{I}{2} + j - k + 2 \right) A(j,k). \end{aligned} \quad (104)$$

For the distributions of  $\mathcal{R}_X^{(n, \frac{I}{2})}$ , see the right of Fig. 9. Obviously, the distribution of points of the same color forms a quasifuzzy four-sphere. (The distribution of  $\mathcal{R}_X^{(n,s)}$  is illustrated in Fig. 7 with  $X_5$  as the vertical axis.) At  $I \rightarrow \infty$  and  $|s| \ll I$ , we have

$$\mathcal{R}_X^{(n,s)} \rightarrow 1 \quad \left( B(j,k) \rightarrow \frac{1}{2} I^2 \right). \quad (105)$$

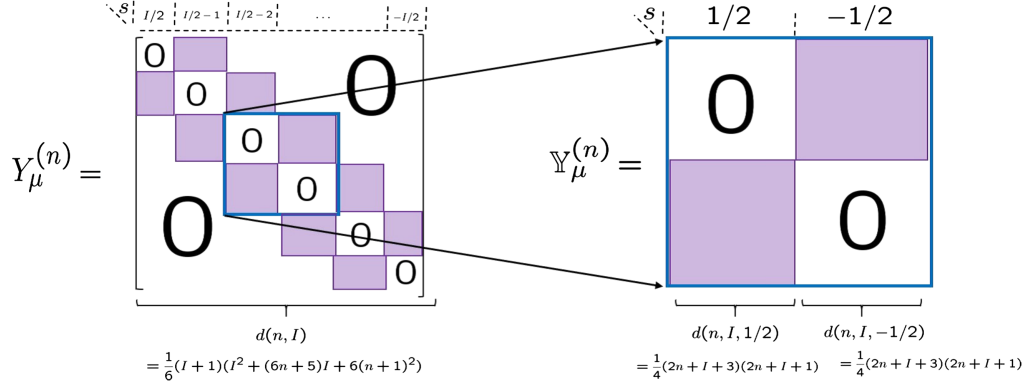
When  $I$  is even,  $\mathcal{R}_X^{(n,s)}$  takes the maximum value at  $s = j - k = 0$ :

$$\mathcal{R}_X^{(n,s=0)} = \sqrt{\frac{I(I+2)}{(2N+I+4)(2N+I+2)}}. \quad (106)$$

This quantity does not depend on  $n$ , indicating that the equators of all the quasifuzzy four-spheres have the same radius, which is identical to the radius of the fuzzy  $S^4$  (80) (see Fig. 7 also).

## B. Fuzzy three-sphere

The fuzzy three-sphere is naturally embedded within the geometry of the fuzzy four-sphere [18,21,23]. This subspace is composed of  $SO(4)$  representations with


 FIG. 10. The fuzzy three-sphere matrix coordinates  $\mathbb{Y}_\mu^{(n)}$  from  $Y_\mu^{(n)}$  for odd  $I$ .

$s = 1/2 \oplus -1/2$ . In the case of the usual (un-nested) fuzzy four-sphere, there exists only one fuzzy three-sphere around the equator of the fuzzy four-sphere. In contrast, the nested fuzzy four-sphere consists of multiple quasifuzzy four-spheres, each of which accommodates a fuzzy three-sphere. Consequently, the  $N$ th Landau level

fuzzy four-sphere hosts  $N + 1$  fuzzy three-spheres around its equator. To extract the fuzzy three-sphere geometry, we focus on the  $s = 1/2 \oplus -1/2$  subspace of the matrix coordinates  $Y_\mu^{(n)}$ . For odd integer  $I$ , we can derive the fuzzy three-sphere matrix coordinates (see Fig. 10)

$$\mathbb{Y}_\mu^{(n)} = \begin{pmatrix} 0 & \mathcal{Y}_\mu^{(+)}\left(\frac{n}{2} + \frac{I}{4} - \frac{1}{4}, \frac{n}{2} + \frac{I}{4} + \frac{1}{4}\right) \\ \mathcal{Y}_\mu^{(-)}\left(\frac{n}{2} + \frac{I}{4} - \frac{1}{4}, \frac{n}{2} + \frac{I}{4} + \frac{1}{4}\right)^\dagger & 0 \end{pmatrix}, \quad (107)$$

which satisfy

$$\sum_{\mu=1}^4 \mathbb{Y}_\mu^{(n)} \mathbb{Y}_\mu^{(n)} = R_{\mathbb{Y}}^{(n)2} \mathbf{1}_{2d(n, I, 1/2)}, \quad (108)$$

where

$$R_{\mathbb{Y}}^{(n)} \equiv \sqrt{A(j, k)}|_{j=\frac{n}{2}+\frac{I}{4}+\frac{1}{4}, k=\frac{n}{2}+\frac{I}{4}+\frac{1}{4}} = \frac{I+1}{\sqrt{2(2n+I+1)(2n+I+3)}}. \quad (109)$$

Unlike the sum of the squares of  $Y_\mu^{(n)}$  (98), Eq. (108) is proportional to a unit matrix. This implies that while  $Y_\mu^{(n)}$  themselves cannot be regarded as the coordinates of the fuzzy three-sphere, their sub-block matrices  $\mathbb{Y}_\mu^{(n)}$  can be. Furthermore,  $\mathbb{Y}_\mu^{(n)}$  are shown to satisfy

$$\begin{aligned} & [[\mathbb{Y}_\mu^{(n)}, \mathbb{Y}_\nu^{(n)}, \mathbb{Y}_\rho^{(n)}]] \\ &= 8(2n+I+2) \left( \frac{I+1}{(2n+I+1)(2n+I+3)} \right)^2 \epsilon_{\mu\nu\rho\sigma} \mathbb{Y}_\sigma^{(n)}, \end{aligned} \quad (110)$$

where the ‘‘three bracket’’  $[[\mathbb{Y}_\mu, \mathbb{Y}_\nu, \mathbb{Y}_\rho]]$  is defined as

$$[[\mathbb{Y}_\mu^{(n)}, \mathbb{Y}_\nu^{(n)}, \mathbb{Y}_\rho^{(n)}]] \equiv [\mathbb{Y}_\mu^{(n)}, \mathbb{Y}_\nu^{(n)}, \mathbb{Y}_\rho^{(n)}, \Gamma_5] \quad (111)$$

with

$$\Gamma_5 \equiv \begin{pmatrix} \mathbf{1}_{d(n, I, 1/2)} & 0 \\ 0 & -\mathbf{1}_{d(n, I, -1/2)} \end{pmatrix}. \quad (112)$$

Equations (108) and (110) clearly show that  $\mathbb{Y}_\mu^{(n)}$  realize the matrix coordinates of the fuzzy three-sphere.<sup>17</sup> Figure 11

<sup>17</sup>With

$$\mathbb{Y}_5^{(n)} \equiv \frac{I+1}{2} \frac{1}{\sqrt{2(2n+I+3)(2n+I+1)}} \Gamma_5, \quad (113)$$

$\mathbb{Y}_{\mu=1,2,3,4}^{(n)}$  satisfy the orthonormal condition:

$$\text{tr}(\mathbb{Y}_a^{(n)} \mathbb{Y}_b^{(n)}) = \left( \frac{I+1}{4} \right)^2 \delta_{ab}. \quad (114)$$

Equation (110) is realized as a special case of the four-algebra,

$$\begin{aligned} & [\mathbb{Y}_a^{(n)}, \mathbb{Y}_b^{(n)}, \mathbb{Y}_c^{(n)}, \mathbb{Y}_d^{(n)}] \\ &= -2\sqrt{2}(I+1)^3 \frac{2n+I+2}{\sqrt{(2n+I+3)(2n+I+1)^5}} \epsilon_{abcde} \mathbb{Y}_e^{(n)}. \end{aligned} \quad (115)$$

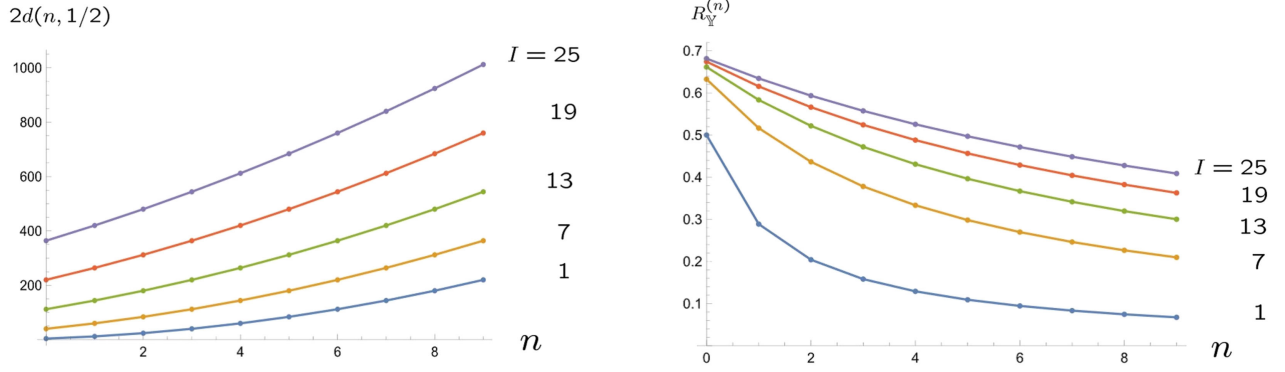


FIG. 11. The matrix size and the radius of the fuzzy three-sphere.

illustrates the behaviors of the matrix sizes and the radii (109) of fuzzy three-spheres. The qualitative features of these quantities are similar to those of the fuzzy four-sphere (Fig. 8) as the fuzzy three-spheres being embedded in of the fuzzy four-sphere. Note that the radius of the fuzzy three-sphere is not equal to that of the fuzzy hyperlatitudes of the same  $s$  (99),  $\mathcal{R}_Y^{(n,s=1/2)} \neq R_V^{(n)}$ , and  $R_V^{(n)}$  does not converge to unity in the continuum limit,  $R_V^{(n)} \xrightarrow{I \rightarrow \infty} 1/\sqrt{2} \neq 1$ .

We also explain how the fuzzy three-sphere itself is obtained within the present noncommutative framework, without referring to the geometry of the fuzzy four-sphere. Since  $S^3$  can be identified with  $SO(4)/SO(3)$ , the stabilizer group  $SO(3)$  is interpreted as the  $SU(2)$  gauge symmetry on the quantum mechanics side. Then, we consider an  $SU(2)$  gauged quantum mechanics on  $S^3$ , known as the  $SO(4)$  Landau model [46,50,54]. In this model,  $n$  represents the Landau level index, and  $s$  signifies the subband index. The  $SO(4)$  Landau model exhibits degeneracy due to the presence of the left-right  $\mathbb{Z}_2$  symmetry, in addition to the global  $SO(4)$  symmetry. The fuzzy three-sphere geometry  $\mathbb{Y}_\mu^{(n)}$  emerges in the lowest energy subbands with

indices  $s = 1/2, -1/2$ , for arbitrary  $n$ th Landau level. The degenerate energy eigenstates that constitute the fuzzy three-sphere consist of the direct sum of irreducible representations of the global symmetry  $SO(4)$ , which is an irreducible representation of the entire symmetry group  $SO(4) \otimes \mathbb{Z}_2$ .

## VI. CONTINUUM LIMIT AND THE $S^4$ GEOMETRY

We discuss the continuum limit and the classical geometry of the nested fuzzy four-sphere. While the continuum limit of the fuzzy two-sphere is the usual classical two-sphere, this is not generally the case for other fuzzy manifolds. For instance, the continuum limit of the un-nested fuzzy  $2k$ -sphere yields the symplectic manifold  $SO(2k+1)/U(k)$  [20], which is obviously distinct from  $S^{2k}$ .

### A. The second Hopf map

The Hopf maps are a key to bridge noncommutative geometry and classical geometry [39]. The second Hopf map

$$\psi_{\alpha=1,2,3,4} \quad (\psi_\alpha^\dagger \psi_\alpha = 1) \in S^7 \rightarrow x_a = \psi_\alpha^* (\gamma_a)_{\alpha\beta} \psi_\beta \in S^4 \quad (x_a x_a = (\psi_\alpha^\dagger \psi_\alpha)^2 = 1) \quad (116)$$

provides a clear understanding of the fuzzy four-sphere geometry. The fuzzification is simply executed by replacing the components of the Hopf spinor with four annihilation operators:

$$\psi_\alpha \rightarrow \frac{1}{\sqrt{I+4}} \hat{\psi}_\alpha, \quad (117)$$

with

$$[\hat{\psi}_\alpha, \hat{\psi}_\beta^\dagger] = \delta_{\alpha\beta}, \quad [\hat{\psi}_\alpha, \hat{\psi}_\beta] = 0. \quad (118)$$

The ‘‘quantized’’ Hopf map is now given by

$$\hat{\psi}_\alpha \quad (\hat{\psi}_\alpha^\dagger \hat{\psi}_\alpha = I) \rightarrow X_a = \frac{1}{I+4} \hat{\psi}_\alpha^\dagger (\gamma_a)_{\alpha\beta} \hat{\psi}_\beta, \quad (119)$$

which satisfy

$$X_a X_a = \frac{1}{(I+4)^2} (\hat{\psi}_\alpha^\dagger \hat{\psi}_\alpha) (\hat{\psi}_\beta^\dagger \hat{\psi}_\beta + 4) = \frac{I}{I+4}. \quad (120)$$

Notice that  $X_a$  (119) coincide with the lowest Landau level coordinate operators (70). The total manifold  $S^7$  represents the classical manifold of the Hopf spinor and the  $S^7$  modulo  $U(1)$  phase is  $\mathbb{C}P^3$ , which is the continuum limit of the (un-nested) fuzzy four-sphere. The second Hopf map thus

presents a relationship between the unnested fuzzy four-sphere and its continuum limit.

Also notice that the Hopf spinor for (116) can be chosen as

$$\begin{aligned} \psi &= \frac{1}{\sqrt{2(1+x_5)}} \begin{pmatrix} 1+x_5 \\ 0 \\ x_4-ix_3 \\ x_2-ix_1 \end{pmatrix} \\ &= \begin{pmatrix} \cos \frac{\xi}{2} \\ 0 \\ \sin \frac{\xi}{2} (\cos \chi - i \sin \chi \cos \theta) \\ -i \sin \frac{\xi}{2} \sin \chi \sin \theta e^{i\phi} \end{pmatrix}, \end{aligned} \quad (121)$$

which satisfies

$$\sum_{a=1}^5 x_a \gamma_a \psi = +\psi. \quad (122)$$

This is the simplest version of the  $SO(5)$  spin-coherent state equation, which plays a central role in deriving the classical geometry of the fuzzy four-sphere in Sec. VIC 1.

### B. Continuum limit

To expand a concrete discussion, let us focus on the north point of the nested fuzzy four-sphere. Since the nested fuzzy four-sphere is an  $SO(5)$  symmetric object, we can choose the north pole as a reference point without loss of generality. The north pole is represented by the index  $s = I/2$ , which corresponds to the  $N + 1$  most right edges of the oblique  $SO(4)$  lines in Fig. 3:

$$\bigoplus_{n=0}^N (j, k)|_{s=I/2} = \bigoplus_{n=0}^N \left( \frac{I}{2} + \frac{n}{2}, \frac{n}{2} \right)_4. \quad (123)$$

Since  $j$  and  $k$  are two independent  $SU(2)$  indices, the  $(j, k)_4$  realizes a direct product of two fuzzy spheres specified by the  $SU(2)$  spins,  $j$  and  $k$ , in the language of the fuzzy geometry. In the continuum limit  $I \rightarrow \infty$ , Eq. (123) becomes

$$\bigoplus_{n=0}^N (j, k)|_{s=I/2} \sim \bigoplus_{n=0}^N \left( \frac{I}{2}, 0 \right), \quad (124)$$

which suggests that the fuzzy structure of the north pole is well approximated by the  $N + 1$  identical fuzzy two-spheres, each with the  $SU(2)$  spin  $I/2$ . Since every  $SO(4)$  line or quasifuzzy four-sphere thus accommodates a fuzzy two-sphere, each quasifuzzy four-sphere is described locally by  $S^4 \times S^2$ , or  $\mathbb{C}P^3$  in the continuum. Consequently, the nested fuzzy four-sphere is reduced to

$N + 1$  overlapped identical  $\mathbb{C}P^3$ s. This is also suggested by the continuum limit of the degeneracy (45)

$$D(N, I) \xrightarrow{I \rightarrow \infty} (N + 1) \cdot \frac{1}{6} I^3, \quad (125)$$

where  $\frac{1}{6} I^3$  denotes the degrees of freedom of a single fuzzy  $\mathbb{C}P^3$ .

It should be emphasized that while the continuum limit of the nested fuzzy four-sphere is  $N + 1$  overlapped  $\mathbb{C}P^3$ s, their fuzzification does not recover the original nested fuzzy four-sphere but just provides  $N + 1$  identical fuzzy  $\mathbb{C}P^3$ s (or  $N + 1$  unnested identical fuzzy four-spheres). In other words, the nested fuzzy four-sphere geometry cannot be reproduced from its corresponding continuum manifold. This agrees with the previous observation that the nested fuzzy four-sphere is a pure quantum object.

### C. $S^4$ geometry

The coherent state method [88–90] and the probe brane method [91–93] are systematic methods to obtain a classical manifold corresponding to a given matrix geometry. These two methods are related but not exactly the same [60,93]. Here, we derive the  $S^4$  geometry from the matrix coordinates using these methods.

#### 1. Coherent state method

For matrix coordinates  $X_a$ , the coherent method [88–90] adopts the following matrix Hamiltonian,

$$H = \sum_{a=1}^5 (X_a^{[N]} - x_a \mathbf{1}_{D(N,I)})^2. \quad (126)$$

We can derive classical manifold as a configuration of  $x_a$  by following the three steps: First, we diagonalize the matrix Hamiltonian to derive the groundstate energy  $E_G(x_a)$ . Second, we examine the minimum of  $E_G(x_a)$  as a function of  $x_a$  to determine the vacuum manifold of  $x_a$ . Last, we take the  $I \rightarrow \infty$  limit of this configuration.

The matrix Hamiltonian (126) is rewritten as

$$\begin{aligned} H &= X_a^{[N]2} - 2x_a X_a^{[N]} + r^2 \mathbf{1}_{D(N,I)} \\ &= \left( \frac{I(I+2)}{(2N+I+4)(2N+I+2)} + r^2 \right) \mathbf{1}_{D(N,I)} - 2x_a X_a^{[N]}, \end{aligned} \quad (127)$$

with

$$r \equiv \sqrt{x_a x_a}. \quad (128)$$

The cross term of Eq. (127) is diagonalized as

$$U(\xi, \chi, \theta, \phi)^\dagger (x_a X_a^{[N]}) U(\xi, \chi, \theta, \phi) = r X_5^{[N]}, \quad (129)$$

where

$$\begin{aligned} U(\xi, \chi, \theta, \phi) &\equiv H(\chi, \theta, \phi)^\dagger e^{i\xi\Sigma_{45}^{[N]}} H(\chi, \theta, \phi) \\ (H(\chi, \theta, \phi) &\equiv e^{-i\chi\Sigma_{34}^{[N]}} e^{i\theta\Sigma_{31}^{[N]}} e^{i\phi\Sigma_{12}^{[N]}}). \end{aligned} \quad (130)$$

The maximal eigenvalue of  $X_5^{[N]}$  is attained at the north pole  $s = I/2$  of the outermost quasifuzzy four-sphere  $n = N$  with degeneracy  $d(N, I, s = I/2)$ :

$$X_5^{[N]} \mathbf{e}_\sigma = \frac{I}{2N + I + 4} \mathbf{e}_\sigma \quad (\sigma = 1, 2, \dots, d(N, I, I/2)). \quad (131)$$

Here,  $\mathbf{e}_\sigma$  denotes a  $D(N, I)$ -component unit vector with  $(\mathbf{e}_\sigma)_\alpha = \delta_{\sigma\alpha}$ . The  $SO(5)$  rotation of  $\mathbf{e}_\sigma$  to align with the direction of  $x_a$  will result in

$$(x_a X_a^{[N]}) \Psi_\sigma^{[N, I]} = r \frac{I}{2N + I + 4} \Psi_\sigma^{[N, I]}, \quad (132)$$

where

$$\Psi_\sigma^{[N, I]}(\xi, \chi, \theta, \phi) \equiv U(\xi, \chi, \theta, \phi) \mathbf{e}_\sigma = \begin{pmatrix} U_{1, \sigma} \\ U_{2, \sigma} \\ \vdots \\ U_{D, \sigma} \end{pmatrix}. \quad (133)$$

Equation (132) signifies a generalized  $SO(5)$  spin-coherent state equation and its simplest version ( $N = 0, I = 1$ ) corresponds to Eq. (122).<sup>18</sup> The spin-coherent states (133) constitute an orthonormal set:<sup>19</sup>

$$\Psi_\sigma^{[N, I]}(\xi, \chi, \theta, \phi)^\dagger \Psi_\tau^{[N, I]}(\xi, \chi, \theta, \phi) = \delta_{\sigma\tau}. \quad (135)$$

The ground state energy is then obtained as

$$E_G(r) = r^2 - 2r \frac{I}{2N + I + 4} + \frac{I(I+2)}{(2N + I + 4)(2N + I + 2)}, \quad (136)$$

<sup>18</sup>From (132), we have

$$\Psi_\sigma^{[N, I] \dagger} X_a^{[N]} \Psi_\sigma^{[N, I]} = r \frac{I}{2N + I + 4} x_a. \quad (134)$$

This concise form of the transformation from matrix coordinates  $X_a$  to classical coordinates  $x_a$  is given in Ref. [62].

<sup>19</sup>The  $SO(5)$  spin-coherent states are closely related to the  $SO(5)$  Landau level eigenstates (35), as both are realized in the unitary matrix (130) [57]. See Ref. [94] for more details.

and the corresponding eigenstates are given by (133) with degeneracy

$$d(N, I, I/2) = (N + 1)(N + I + 1). \quad (137)$$

The classical vacuum of  $E_G(r)$  (136) is attained by

$$r = \frac{I}{2N + I + 4}. \quad (138)$$

Note that Eq. (138) is equal to the radius of the outermost quasifuzzy four-sphere  $n = N$  (93). From (138), we have

$$\lim_{I \rightarrow \infty} r = 1. \quad (139)$$

We thus obtained the classical  $S^4$  geometry ( $x_a x_a = 1$ ) from  $X_a^{[N]}$ .

## 2. Probe brane method

The probe brane method [91–93] adopts the Dirac-operator matrix

$$D(x_a) = \sum_{a=1}^5 \gamma_a \otimes (X_a^{[N]} - x_a \mathbf{1}_{D(N, I)}). \quad (140)$$

In this method, the classical manifold is obtained through the following two steps. First, we consider the condition for the existence of the zero modes of the Dirac-operator matrix (140). For zero modes to exist,  $x_a$  must satisfy a certain condition which characterizes a classical manifold. Subsequently, we take  $I \rightarrow \infty$  limit of the classical manifold to derive the corresponding classical geometry. Due to the tensor product form of (140), it is rather technically intricate to derive general results unlike the case of the coherent state method. Hence, we conduct numerical investigations by employing the explicit forms of  $X_a^{[N]}$ . The obtained numerical results imply

$$\det(D(x_a))|_{x_a x_a = \left(\frac{I}{2N + I + 4}\right)^2} = 0 \quad (141)$$

and the number of the zero modes

$$d(N, I + 1, (I + 1)/2) = (N + 1)(N + I + 2). \quad (142)$$

Equation (141) indicates that the zero modes exist when  $x_a$  satisfy  $r = \frac{I}{2N + I + 4}$ , which is equal to the previous result (138). Therefore, both the coherent state method and the probe brane method yield the identical classical geometry in the present case. Meanwhile, the number of the zero modes (142) is distinct from that of the coherent states (137).

## VII. REALIZATION IN YANG-MILLS MATRIX MODELS

In this section, we demonstrate that the nested fuzzy four-spheres realize new classical solutions of Yang-Mills matrix models and investigate their physical properties. In particular, we clarify distinct behaviors between the lowest Landau level matrix geometry and the newly obtained higher Landau level matrix geometries.

### A. Basic relations

Using the explicit forms of  $X_a^{[N]}$ , we can demonstrate that  $X_a^{[M]}$  satisfy

$$X_a^{[N]} X_a^{[N]} = c_1(N, I) \mathbf{1}_{D(N, I)}, \quad (143a)$$

$$X_b^{[N]} X_a^{[N]} X_b^{[N]} = c_2(N, I) X_a^{[N]}, \quad (143b)$$

$$\epsilon_{abcde} X_b^{[N]} X_c^{[N]} X_d^{[N]} X_e^{[N]} = -4! c_3(N, I) X_a^{[N]}, \quad (143c)$$

where  $c_1$  and  $c_3$  are given by (77) and (83), respectively. In principle, we can determine all of values of the  $c_s$  through Eq. (143). For instance,  $c_2(1, 1) = -\frac{47}{1225}$ ,  $c_2(1, 2) = \frac{5}{72}$ ,  $c_2(1, 3) = \frac{211}{1323}$ ,  $c_3(1, 1) = \frac{181}{128625}$ ,  $c_3(1, 2) = \frac{31}{20736}$ ,  $c_3(1, 3) = \frac{367}{250047}$ .<sup>20</sup> Equations (143a) and (143b) imply

$$\text{radius: } \hat{R} \equiv \frac{c_1^{1/2}}{c_3^{1/3}} \quad (\hat{X}_a^{[M]} \hat{X}_a^{[M]} = \hat{R}^2 \mathbf{1}_{D(N, I)}), \quad (150a)$$

$$\text{potential energy: } \hat{V} = -\frac{1}{4} \text{tr}([\hat{X}_a^{[M]}, \hat{X}_b^{[M]}]^2) = \frac{1}{2c_3^{4/3}} (c_1 - c_2) c_1 D(N, I), \quad (150b)$$

$$\text{potential energy density: } \frac{\hat{V}}{\hat{R}^4} = -\frac{1}{4} \text{tr}([\hat{X}_a^{[M]}, \hat{X}_b^{[M]}]^2) = \frac{c_1 - c_2}{2c_1} D(N, I). \quad (150c)$$

The quantities in Eq. (150) are plotted in Fig. 13. The radius  $\hat{R}$  increases as  $N$  increases (Fig. 13) unlike the original  $R$  (80) (Fig. 8). The behaviors of the quantities in Eq. (150) are qualitative similar to those of the fuzzy two-sphere (Fig. 17), except for the potential energy densities

<sup>20</sup>In the lowest Landau level ( $N = 0$ ), the coefficients are given by

$$\begin{aligned} c_1(0, I) &= \frac{I}{I+4}, & c_2(0, I) &= \frac{I^2 + 4I - 8}{(I+4)^2}, \\ c_3(0, I) &= \frac{I+2}{3(I+4)^3}. \end{aligned} \quad (144)$$

$$-\frac{1}{4} ([X_a^{[M]}, X_b^{[M]}]^2) = \frac{1}{2} (c_1 - c_2) c_1 \mathbf{1}_{D(N, I)} \quad (145)$$

and the potential energy is expressed as

$$V(X_a^{[M]}) \equiv -\frac{1}{4} \text{tr}([X_a^{[M]}, X_b^{[M]}]^2) = \frac{1}{2} (c_1 - c_2) c_1 D(N, I). \quad (146)$$

The behaviors of the  $c_s$  and the  $V$  are illustrated in Fig. 12. Their behaviors are similar to those of the fuzzy two-sphere (see Fig. 16 in Appendix B).

While we have utilized  $X_a^{[M]}$  as the matrix coordinates, from an algebraic standpoint, it might be more natural to adopt “normalized” matrix coordinates that align with the quantum Nambu algebra:

$$[\hat{X}_a^{[M]}, \hat{X}_b^{[M]}, \hat{X}_c^{[M]}, \hat{X}_d^{[M]}] = -4! \epsilon_{abcde} \hat{X}_e^{[M]}, \quad (147)$$

or

$$\hat{X}_a^{[M]} = \frac{1}{c_3^{1/3}} X_a^{[M]}. \quad (148)$$

For  $\hat{X}_a^{[M]}$ , important physical quantities are given by<sup>21</sup>

(the lower right of Fig. 13) in which the order of magnitudes for  $I = 1, 2, 3$  is reversed between the lowest Landau level ( $N = 0$ ) and the higher Landau levels ( $N \geq 1$ ).

<sup>21</sup>In the lowest Landau level ( $N = 0$ ), Eq. (148) is reduced to  $\hat{X}_a^{[0]} = (\frac{3}{I+2})^{1/3} (I+4) X_a^{[0]} = (\frac{3}{I+2})^{1/3} \Gamma_a$ , and Eq. (150) becomes

$$\begin{aligned} \hat{R} &= I^{1/2} (I+4)^{1/2} \left( \frac{3}{I+2} \right)^{1/3}, \\ V &= 2 \left( \frac{3}{I+2} \right)^{1/3} I(I+1)(I+3)(I+4), \\ \frac{V}{\hat{R}^4} &= \frac{2(I+1)(I+2)(I+3)}{3(I+4)}. \end{aligned} \quad (149)$$

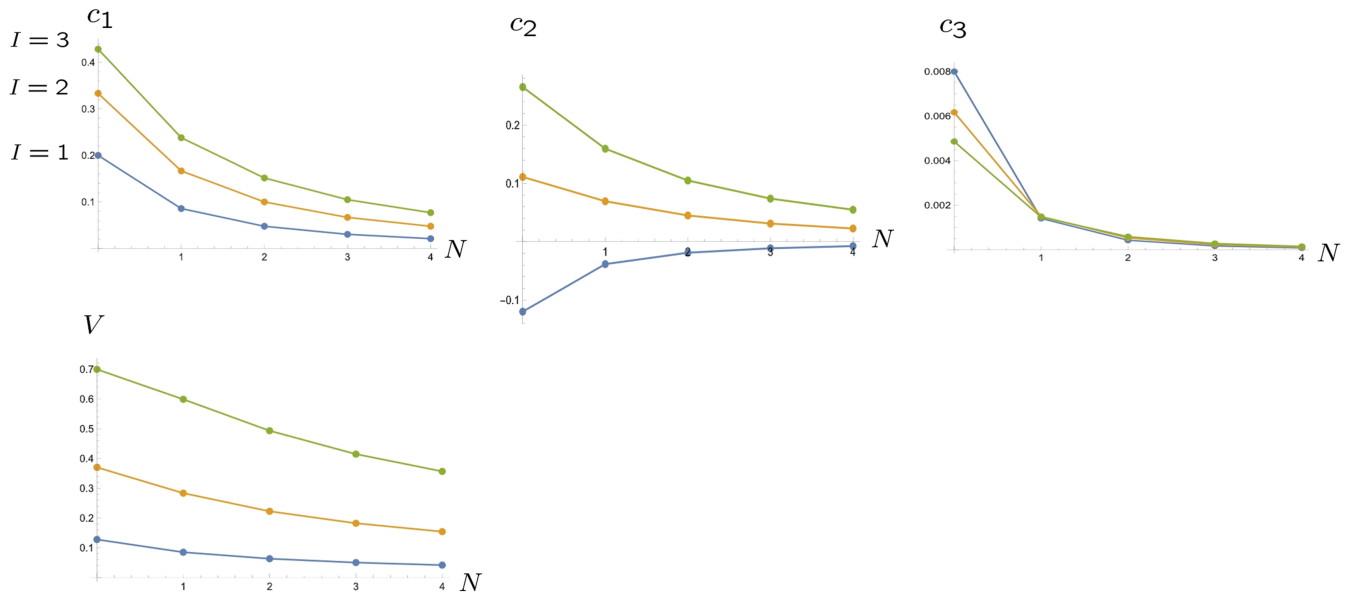


FIG. 12. The upper: the behaviors of  $c_s$ . The blue, orange, and green lines correspond to  $I = 1, 2, 3$ , respectively. The lower: the behaviors of the potential (146).

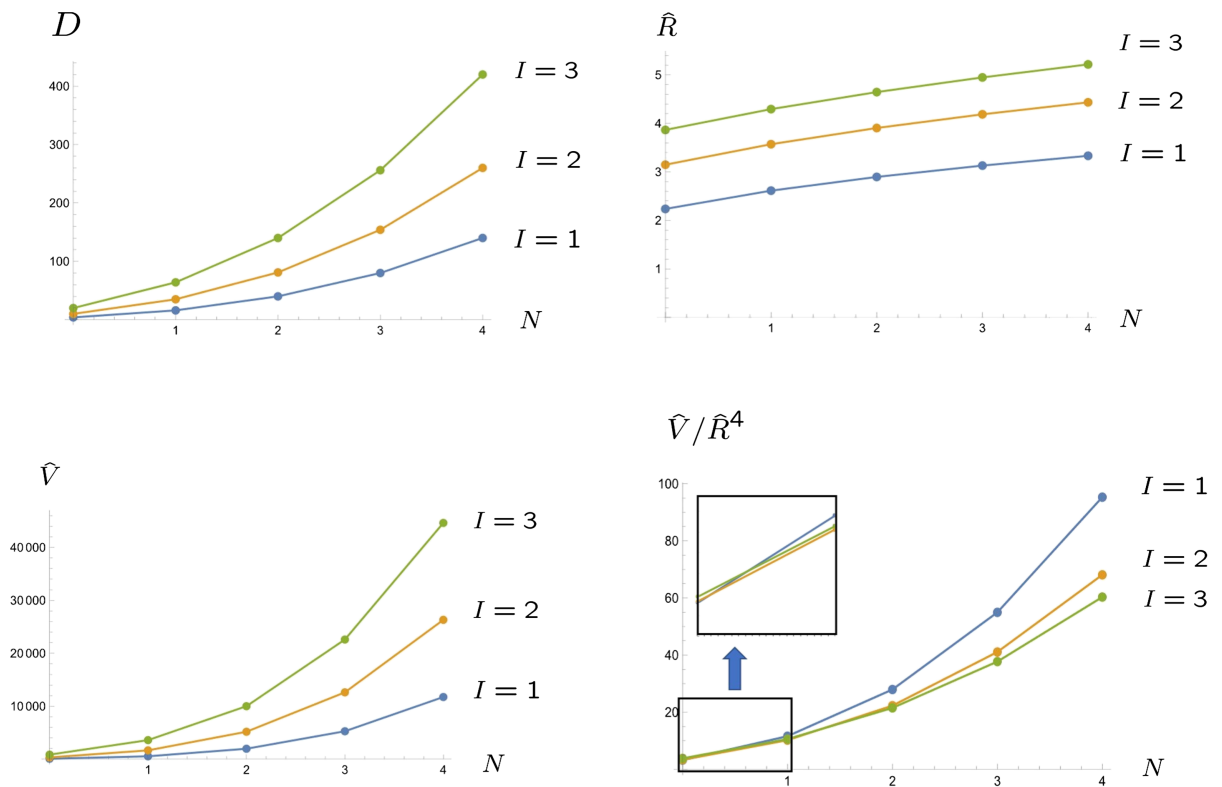


FIG. 13. Behaviors of the matrix size  $D$  (the upper left), the radius (the upper right), and the potential energy (the lower left) and the potential energy density (the lower right).

## B. As classical solutions of Yang-Mills matrix models

### 1. With a mass term

Let us consider Yang-Mills matrix model with a mass term [95]:

$$S_{\text{mass}} = -\frac{1}{4}\text{tr}([A_a, A_b]^2) - \frac{1}{2}\rho \text{tr}(A_a^2) \quad (\rho > 0). \quad (151)$$

Under the scaling  $A_i \rightarrow \sqrt{\rho}A_i$ , the parameter  $\rho$  turns to the overall scale factor of the action and does not have any physical effect. We will take  $\rho = 1$ :

$$S_{\text{mass}} = -\frac{1}{4}\text{tr}([A_a, A_b]^2) - \frac{1}{2}\text{tr}(A_a^2). \quad (152)$$

The equations of motion are derived as

$$[[A_a, A_b], A_b] = A_a. \quad (153)$$

Using (143), we readily see that the nested fuzzy four-spheres realize new classical solutions:<sup>22</sup>

$$A_a^{\text{cl}} = \alpha_{\text{mass}}(N, I) \hat{X}_a^{[N]}, \quad (154)$$

where the noncommutative parameter is given by

$$\alpha_{\text{mass}}(N, I) \equiv \frac{c_3(N, I)^{1/3}}{\sqrt{2(c_1(N, I) - c_2(N, I))}}. \quad (155)$$

The noncommutative parameter  $\alpha$  is a parameter-dependent quantity unlike the case of the fuzzy two-sphere solution (see Appendix B 2). This brings specific physical properties to the fuzzy four-sphere solutions. The physical quantities (150) are evaluated as<sup>23</sup>

$$\text{radius: } R_{\text{mass}} \equiv \sqrt{\frac{c_1}{2(c_1 - c_2)}} \quad (A_a^{\text{cl}} A_a^{\text{cl}} = R_{\text{mass}}^2 \mathbf{1}), \quad (157a)$$

$$\begin{aligned} \text{action: } S_{\text{mass}}^{\text{cl}} &= \left(-\frac{1}{4} + \frac{1}{2}\right) \text{tr}([A_a^{\text{cl}}, A_b^{\text{cl}}]^2) = \frac{1}{4} \text{tr}([A_a^{\text{cl}}, A_b^{\text{cl}}]^2) \\ &= -\frac{1}{8} \frac{c_1}{c_1 - c_2} D = -\frac{1}{4} R_{\text{mass}}^2 D, \end{aligned} \quad (157b)$$

<sup>22</sup>Fuzzy two-sphere and fuzzy torus are also solutions of Eq. (153) [95].

<sup>23</sup>In the lowest Landau level ( $N = 0$ ), Eq. (157) is reduced to

$$\begin{aligned} R_{\text{mass}} &= \frac{1}{4} \sqrt{I(I+4)}, \\ S_{\text{mass}}^{\text{cl}} &= -\frac{1}{384} I(I+1)(I+2)(I+3)(I+4), \\ \frac{S_{\text{mass}}^{\text{cl}}}{R_{\text{mass}}^4} &= -\frac{2}{3} \frac{(I+1)(I+2)(I+3)}{I(I+4)}. \end{aligned} \quad (156)$$

$$\text{action density: } \frac{S_{\text{mass}}^{\text{cl}}}{R_{\text{mass}}^4} = -\frac{c_1 - c_2}{2c_1} D = -\frac{1}{4R_{\text{mass}}^2} D = -\frac{V}{\hat{R}^4}. \quad (157c)$$

The behaviors of Eqs. (155) and (157) are shown in Fig. 14. Similar to the case of  $\hat{X}_a^{[N]}$  in Sec. VII A, the action densities (the lower right of Fig. 14) exhibit qualitatively distinct behaviors to the fuzzy two-sphere (Fig. 17).

### 2. With a fifth-rank Chern-Simons term

We next consider the Yang-Mills matrix model with a fifth-rank Chern-Simons term [95]

$$S_{\text{CS}}[X_a] = -\frac{1}{4}\text{tr}([X_a, X_b]^2) + \frac{\lambda}{5} \epsilon_{abcde} \text{tr}(X_a X_b X_c X_d X_e). \quad (158)$$

The coupling constant  $\lambda$  can be absorbed in the action when scaling  $A_a$  as  $A_a \rightarrow \frac{1}{\lambda} \cdot A_a$ . We then set  $\lambda = 1$  and deal with the following action:

$$S_{\text{CS}} = -\frac{1}{4}\text{tr}([A_a, A_b]^2) + \frac{1}{5} \epsilon_{abcde} \text{tr}(A_a A_b A_c A_d A_e). \quad (159)$$

The equations of motion are given by

$$[[A_a, A_b], A_b] = -\epsilon_{abcde} A_b A_c A_d A_e. \quad (160)$$

From (143), we easily obtain new classical solutions as

$$A_a^{\text{cl}} = \alpha_{\text{CS}}(N, I) \hat{X}_a^{[N]}, \quad (161)$$

with

$$\alpha_{\text{CS}}(N, I) \equiv \frac{1}{12} \frac{c_1(N, I) - c_2(N, I)}{c_3(N, I)^{2/3}}, \quad (162)$$

and<sup>24</sup>

<sup>24</sup>In the lowest Landau level ( $N = 0$ ), we have

$$\alpha = \frac{2}{3} \left(\frac{3}{I+2}\right)^{2/3}, \quad A_a^{\text{cl}} = \alpha \hat{X}_a^{[0]} = \frac{2}{I+2} \Gamma_a, \quad (163)$$

which satisfies

$$[A_a^{\text{cl}}, A_b^{\text{cl}}, A_c^{\text{cl}}, A_d^{\text{cl}}] = -\left(\frac{8}{I+2}\right)^2 \epsilon_{abcde} A_e^{\text{cl}}. \quad (164)$$

Equation (166) reproduces the results of Ref. [95] for  $N = 0$ :

$$\begin{aligned} R_{\text{CS}} &= \frac{2\sqrt{I(I+4)}}{I+2}, \quad S_{\text{CS}}^{\text{cl}} = \frac{32I(I+1)(I+3)(I+4)}{15(I+2)^3}, \\ \frac{S_{\text{CS}}^{\text{cl}}}{R_{\text{CS}}^4} &= \frac{2}{15} \frac{(I+1)(I+2)(I+3)}{I(I+4)}. \end{aligned} \quad (165)$$

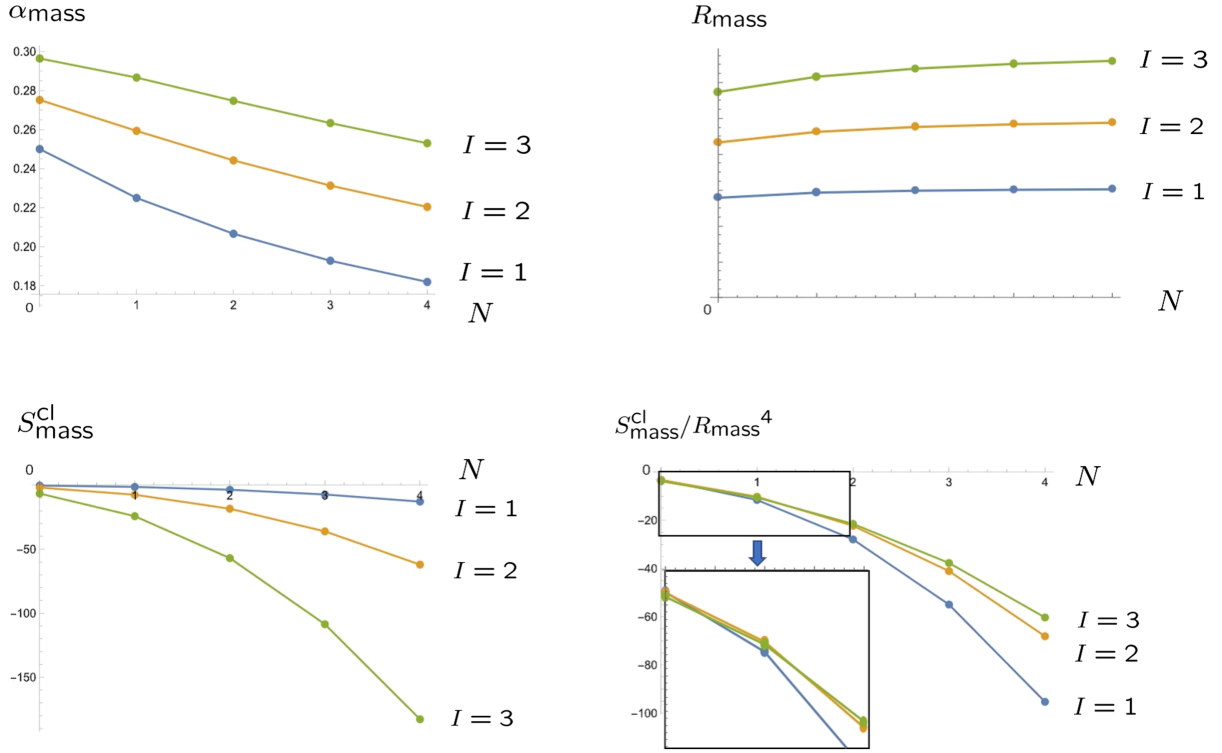


FIG. 14. Behaviors of Eqs. (155) and (157).

$$\text{radius: } R_{\text{CS}} \equiv \frac{1}{12} \frac{(c_1 - c_2)c_1^{1/2}}{c_3} = \alpha_{\text{CS}} \hat{R} \quad (A_a^{\text{cl}} A_a^{\text{cl}} = \alpha_N^2 \hat{X}_a^{[N]} \hat{X}_a^{[N]} = R_{\text{CS}}^2 \mathbf{1}_{D(N,I)}), \quad (166a)$$

$$\text{action: } S_{\text{CS}}^{\text{cl}} \equiv S_{\text{CS}}[A_a^{\text{cl}}] = -\overbrace{\left(\frac{1}{4} - \frac{1}{5}\right)}^{\frac{1}{20}} \text{tr}([A_a^{\text{cl}}, A_b^{\text{cl}}]^2) = \frac{1}{5} \alpha_{\text{CS}}^4 V = \frac{1}{10} \frac{(c_1 - c_2)^5 c_1}{(12c_3)^4} D(N, I), \quad (166b)$$

$$\text{action density: } \frac{S_{\text{CS}}^{\text{cl}}}{R_{\text{CS}}^4} = \frac{1}{10} \frac{c_1 - c_2}{c_1} D(N, I) = \frac{1}{5} \frac{V}{\hat{R}_{\text{CS}}^4} = -\frac{1}{5} \frac{S_{\text{mass}}^{\text{cl}}}{R_{\text{mass}}^4}. \quad (166c)$$

Figure 15 depicts the behaviors of Eq. (166). There are three noteworthy points. First, the order of  $\alpha_{\text{CS}}$  for  $I = 1, 2, 3$  is the reverse of that of  $\alpha_{\text{mass}}$  (the upper left in Fig. 14). Second, the order of magnitudes of  $R_{\text{CS}}$  for  $I = 1, 2, 3$  is reversed between  $N = 0$  and  $N = 2$ . Last, the order of magnitudes of both  $S_{\text{CS}}^{\text{cl}}$  (lower left in Fig. 15) and  $S_{\text{CS}}^{\text{cl}}/R_{\text{CS}}^4$  (lower right in Fig. 15) of  $N = 0$  for  $I = 1, 2, 3$  is the reverse of those of  $N \geq 1$ . Thus, the lowest Landau level matrix geometry ( $N = 0$ ) and the newly obtained higher Landau level matrix geometries ( $N \geq 1$ ) exhibit qualitatively distinct physical properties. It is rather curious that, while the matrix size  $D$  is a monotonically increasing function about  $I$  and the quantities such as  $R_{\text{CS}}$  and  $S_{\text{CS}}^{\text{cl}}$  are expected to show similar behaviors the higher Landau level

matrix geometries, i.e., the nested fuzzy four-spheres, do not follow this anticipation.

## VIII. EVEN HIGHER DIMENSIONS

We here investigate higher Landau level matrix geometries in even higher dimensions. The associated higher form gauge field and Yang-Mills matrix model are also discussed.

### A. Landau level matrix geometries

It is known that (unnested) higher dimensional fuzzy spheres are realized as the lowest Landau level matrix geometries in higher dimensional Landau models

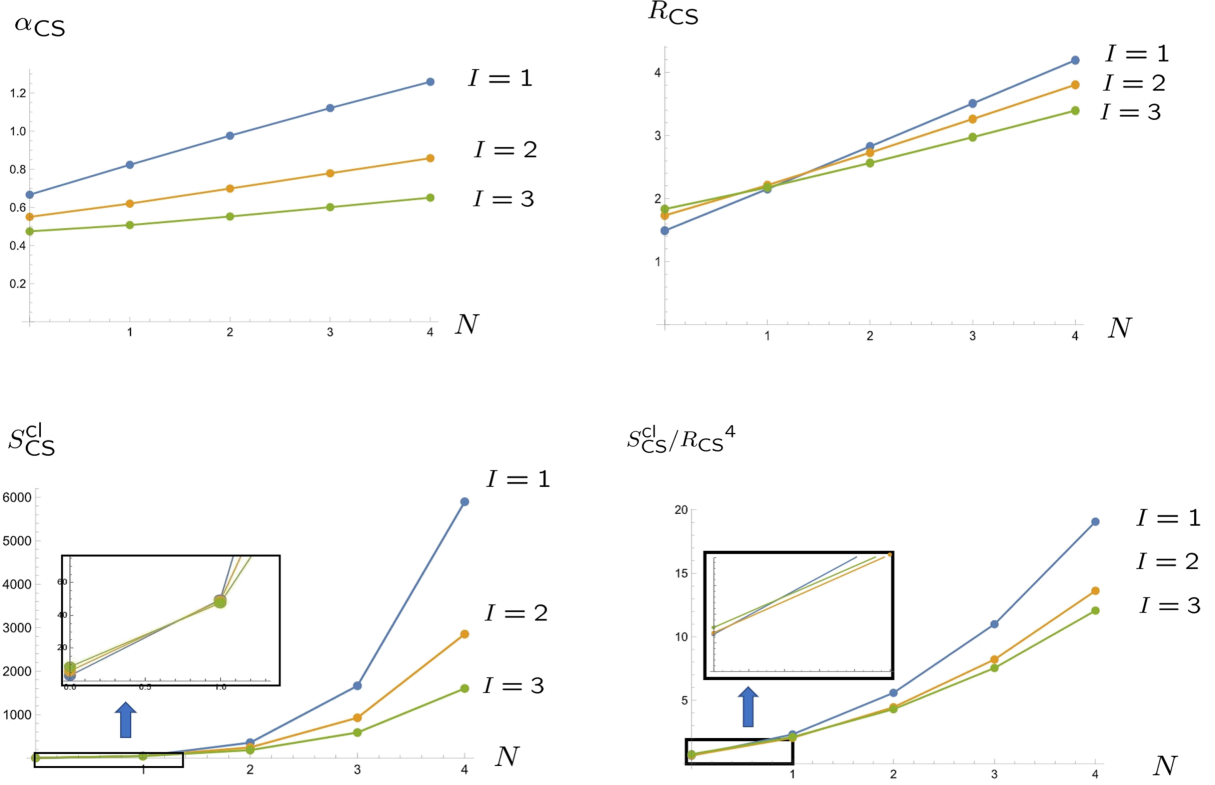


FIG. 15. Behaviors of the noncommutative scale (the upper left), the radius (the upper right), the action (the lower left), and the action density (the lower right).

[44,75,96]. Since  $S^d \simeq SO(d+1)/SO(d)$ , the corresponding gauged quantum mechanics is given by the  $SO(d+1)$  Landau model in the  $SO(d)$  non-Abelian monopole background. The matrix coordinates in the lowest Landau level are given by the fully symmetric combination of the  $SO(2k+1)$  gamma matrices:

$$X_a^{[N=0]} = \frac{1}{I+2k} (\gamma_a \otimes 1 \otimes \cdots \otimes 1 + 1 \otimes \gamma_a \otimes \cdots \otimes 1 + \cdots + 1 \otimes 1 \otimes \cdots \otimes \gamma_a)_{\text{sym}}, \quad (167)$$

which satisfy the  $\text{Spin}(2k+2)$  Lie algebraic commutation relations together with the  $SO(2k)$  generators.

The higher Landau level geometries in the  $SO(d+1)$  Landau model have not been investigated so far. Though it is in principle possible to derive higher Landau level matrix geometries by following the present noncommutative

scheme, it is rather laborious to solve the eigenvalue problem of the higher dimensional Landau Hamiltonian. Furthermore, the resulting matrix structures may be mathematically too involved to deduce useful information about the higher dimensional noncommutative geometry. Therefore, we will engage in a somewhat speculative yet more general discussion based on group theory. Let us focus on the following  $SO(2k+1)$  irreducible representation

$$[l_1, l_2, \dots, l_k]_{SO(2k+1)} = [N+I, I, \dots, I], \quad (168)$$

which corresponds to the  $N$ th Landau level eigenstates of the  $SO(2k+1)$  Landau model studied in Refs. [44,75]. From group representation theory, the corresponding degeneracy is given by

$$D(N, I)_{SO(2k+1)} = \frac{2N+I+2k-1}{(2k-1)!!} \frac{(N+k-1)! (I+2k-3)!! (N+I+2k-2)!}{N!(k-1)! (I-1)!!} \frac{(N+I+2k-2)!}{(N+I+k-1)!} \prod_{l=1}^{k-2} \frac{(I+2l)!}{(I+l)!} \prod_{l=1}^{k-1} \frac{l!}{(2l)!}. \quad (169)$$

Meanwhile, for the one dimension lower  $SO(2k)$  Landau model, the Landau levels consist of subbands [96]. The eigenstates of the  $s$  band of the  $n$ th Landau level constitute an  $SO(2k)$  irreducible representation:

$$[l_1, l_2, \dots, l_{k-1}, l_k]_{SO(2k)} = \left[ n + \frac{I}{2}, \frac{I}{2}, \dots, \frac{I}{2}, s \right], \quad (170)$$

with degeneracy

$$d(n, I, s)_{SO(2k)} = \frac{(2n + I + 2k - 2)^2 - 4s^2}{4(k-1)^2} \cdot \prod_{2 \leq i \leq k-1} \frac{(n + I + 2k - i - 1)(n + i - 1)}{(2k - i - 1)(i - 1)} \cdot \prod_{2 \leq i < j \leq k-1} \frac{I + 2k - i - j}{2k - i - j} \cdot \prod_{2 \leq i \leq k-1} \frac{(I + 2k - 2i)^2 - 4s^2}{4(k - i)^2}. \quad (171)$$

There exists an exact relation between the degeneracies (169) and (171):

$$D(N, I)_{SO(2k+1)} = \sum_{n=0}^N \sum_{s=-I/2}^{I/2} d(n, I, s)_{SO(2k)}. \quad (172)$$

Equation (172) signifies a higher dimensional generalization of Eq. (45) and implies that the  $SO(2k+1)$  irreducible representation is constructed by adding up the  $SO(2k)$  sectors from  $n = 0$  to  $n = N$  each of which is made of  $s = I/2, \dots, -I/2$ . Since the geometric structure of the fuzzy manifold reflects on the structure of the irreducible representation, the matrix geometry of the  $N$ th Landau level is expected to exhibit  $N + 1$  nested fuzzy structures in arbitrary dimensions, just like the nested fuzzy four-sphere. It is also reasonable to consider that fuzzy  $(2k - 1)$ -spheres are embedded within the nested fuzzy  $2k$ -sphere.

### B. Higher form gauge field and Yang-Mills matrix model

The lowest Landau level matrix geometry in  $2k$  dimension is associated with a generalized Hopf maps [39] and are described by both the  $SO(2k+2)$  Lie algebra and quantum Nambu  $2k$  algebra. Meanwhile, the matrix coordinates in the higher Landau levels are not associated with the generalized Hopf map but are covariant under the  $SO(2k+1)$  transformation like the lowest Landau level matrix coordinates. Therefore, the higher Landau level matrix coordinates will not conform with the Lie algebraic description but instead is described by the quantum Nambu algebra exclusively:

$$[X_{a_1}, X_{a_2}, \dots, X_{a_{2k}}] = (2k)! i^k c_3 \epsilon_{a_1 a_2 \dots a_{2k+1}} X_{2k+1}. \quad (173)$$

When one adopt more general irreducible representations beyond Eq. (168), the corresponding fuzzy manifold will exhibit a more exotic quantum geometry than the nested fuzzy structure, however, due to the existence of the  $SO(2k+1)$  covariance, the matrix coordinates will also adhere to the quantum Nambu algebra (173).

Interestingly, “magnetic field” appears on the right-hand side of (173) [75], which signifies the tensor monopole field strength:

$$G_{2k} = \frac{1}{2^{k+1} r^{2k+1}} \epsilon_{a_1 a_2 \dots a_{2k+1}} x_{a_{2k+1}} dx_{a_1} \wedge dx_{a_2} \wedge \dots \wedge dx_{a_{2k}}. \quad (174)$$

The existence of the higher form gauge field behind the quantum Nambu geometry is thus glimpsed. One may wonder where such a higher gauge symmetry comes from, where as the present quantum mechanical system only has the  $SO(2k)$  gauge symmetry. Indeed, the tensor monopole gauge field is directly obtained from the  $SO(2k)$  monopole gauge field through the Chern-Simons term [75].

The (unnested) fuzzy  $2k$ -sphere realizes a solution of [22]

$$[[X_a, X_b], X_c] = i^k \epsilon_{a a_2 a_3 \dots a_{2k+1}} X_{a_2} X_{a_3} \dots X_{a_{2k+1}}, \quad (175)$$

which is derived from the Yang-Mills matrix model with a  $2k + 1$  rank Chern-Simons term,

$$S_{CS}[X_a] = -\frac{1}{4} \text{tr}([X_a, X_b]^2) - i^k \frac{1}{2k+1} \text{tr}(\epsilon_{a_1 a_2 \dots a_{2k+1}} X_{a_1} X_{a_2} \dots X_{a_{2k+1}}). \quad (176)$$

Since the equations of motion are concerned with the covariance of the matrix coordinates, it is anticipated that the nested fuzzy  $2k$ -spheres realize classical solutions of Eq. (175). The action of for the fuzzy  $2k$ -sphere solution is given by

$$S_{CS}(X_a = X_a^{\text{cl}}) = \left( -\frac{1}{4} + \frac{1}{2k+1} \right) \text{tr}([X_a^{\text{cl}}, X_b^{\text{cl}}]^2) = \frac{2k-3}{2k+1} V(X_a^{\text{cl}}), \quad (177)$$

where

$$V(X_a^{\text{cl}}) \equiv -\frac{1}{4} \text{tr}([X_a^{\text{cl}}, X_b^{\text{cl}}]^2). \quad (178)$$

While the signs of  $S_{CS}(X_a^{\text{cl}})$  and  $V(X_a^{\text{cl}})$  are opposite for  $k = 1$ , they have the same sign for  $k \geq 2$ , as we have seen, for  $k = 2$ , in Eq. (166b).

## IX. SUMMARY AND DISCUSSIONS

Based on the insight obtained from the emergent fuzzy geometry in the simple  $SO(3)$  Landau model, we proposed a novel noncommutative scheme for generating the matrix geometries for arbitrary manifolds of the coset type  $G/H$ . In the present approach, manifolds need not be either symplectic or even dimensional unlike the conventional non-commutative schemes. We explicitly derived the matrix geometries for  $S^4$  by utilizing the  $SO(5)$  Landau model. The emergent matrix geometries in higher Landau levels realize pure quantum Nambu geometries in which matrix coordinates are not closed within the canonical formalism of the Lie algebra but are described only by introducing the quantum Nambu algebra. We also demonstrated that such pure quantum matrix geometries manifest new solutions of the Yang-Mills matrix models. The particular features of the nested quantum geometry, such as the internal matrix geometries, continuum limit, and classical counterpart, were clarified. The pure Nambu matrix geometries are common to the higher Landau levels of the Landau models in arbitrary dimensions.

The conventional scheme is based on the spirit of quantization of classical (symplectic) manifolds, i.e., the replacement of the Poisson bracket with the commutator, whereas the present noncommutative scheme is largely based on the mathematical structure of the Hilbert space behind quantum mechanics from the beginning. In this sense, the present scheme is considered to be a quantum-oriented noncommutative scheme. That is the reason why we obtained the pure quantum geometry. We showed this noncommutative scheme is practically useful in deriving novel solutions of the matrix models. As matrix model solutions, the nested matrix geometries exhibit quantitatively distinct behaviors with the unnested fuzzy four-sphere.

The discovery of the novel quantum Nambu matrix geometries now brings various open questions, such as brane construction, relation to tachyon condensation [97,98], realization in the Nahm equation in higher energy physics. The higher form gauge field implied by the quantum Nambu algebra is closely related to the higher Berry phase [99,100] whose usefulness is getting appreciated in the very recent studies of strongly correlated many-body systems. It would be intriguing to speculate on the role of quantum Nambu geometry in condensed matter physics. We also add that the present scheme itself should be appropriately generalized to treat less symmetric fuzzy objects, while we studied highly symmetric objects in this work.

To the best of the author's knowledge, this work is the first example of quantum matrix geometry found in the analysis of the Landau models being practically applied to the solutions of the M(atr)ix models. M(atr)ix theory is assumed to describe the physics at the Planck scale of  $10^{19}$  GeV, while the Landau models or the quantum Hall

effect are about the low temperature physics at millielectron volt. It is rather amazing that same mathematics work in both physics with such a huge energy gap.

## ACKNOWLEDGMENTS

I would like to thank Harold Steinacker for valuable email communications. This work was supported by JSPS KAKENHI Grant No. 21K03542.

## APPENDIX A: GROENEWOLD-MOYAL PLANE FROM PLANAR LANDAU MODEL

We demonstrate a realization of the Groenewold-Moyal plane in higher Landau levels. Let us consider a 2D plane subject to a constant perpendicular magnetic field:

$$\partial_x A_y - \partial_y A_x = B. \quad (\text{A1})$$

We employ the gauge-independent relation (A1), and so all of the following results are also gauge independent. The covariant derivatives and the center-of-mass coordinates are respectively constructed as

$$D_i = \frac{\partial}{\partial x_i} + iA_i, \quad X_i^{\text{CM}} = x_i + i\frac{1}{B}\epsilon_{ij}D_j \quad (i=1,2), \quad (\text{A2})$$

which satisfy two independent commutation relations:

$$[D_x, D_y] = iB, \quad [X^{\text{CM}}, Y^{\text{CM}}] = i\frac{1}{B}, \quad [D_i, X_j^{\text{CM}}] = 0. \quad (\text{A3})$$

We then realize two sets of creation and annihilation operators as

$$a = i\frac{1}{\sqrt{2B}}(D_x - iD_y), \quad a^\dagger = i\frac{1}{\sqrt{2B}}(D_x + iD_y), \\ b = \sqrt{\frac{B}{2}}(X^{\text{CM}} + iY^{\text{CM}}), \quad b^\dagger = \sqrt{\frac{B}{2}}(X^{\text{CM}} - iY^{\text{CM}}), \quad (\text{A4})$$

which satisfy

$$[a, a^\dagger] = [b, b^\dagger] = 1, \quad [a, b] = [a, b^\dagger] = 0. \quad (\text{A5})$$

The Hamiltonian of the planar Landau model is given by

$$H = -\frac{1}{2M}(D_x^2 + D_y^2) = \frac{B}{M}\left(a^\dagger a + \frac{1}{2}\right). \quad (\text{A6})$$

The corresponding energy Landau levels and the eigenstates are

$$E_N = \frac{B}{M}\left(N + \frac{1}{2}\right), \quad |N, m\rangle = \frac{1}{\sqrt{N!m!}} a^{\dagger N} b^{\dagger m} |0\rangle \\ (N, m = 0, 1, 2, \dots). \quad (\text{A7})$$

Using

$$\begin{aligned}x &= X^{\text{CM}} - i\frac{1}{B}D_y = \frac{1}{\sqrt{2B}}(b + b^\dagger) - i\frac{1}{\sqrt{2B}}(a - a^\dagger), \\y &= Y^{\text{CM}} + i\frac{1}{B}D_x = -i\frac{1}{\sqrt{2B}}(b - b^\dagger) + \frac{1}{\sqrt{2B}}(a + a^\dagger),\end{aligned}\quad (\text{A8})$$

we readily evaluate the matrix elements of  $x$  and  $y$ :

$$\begin{aligned}\langle N, m|x|N', m'\rangle &= \frac{1}{\sqrt{2B}}\left(\sqrt{m'}\delta_{m,m'-1} + \sqrt{m'+1}\delta_{m,m'+1}\right)\delta_{N,N'} - i\frac{1}{\sqrt{2B}}\left(\sqrt{N'}\delta_{N,N'-1} - \sqrt{N'+1}\delta_{N,N'+1}\right)\delta_{m,m'}, \\ \langle N, m|y|N', m'\rangle &= -i\frac{1}{\sqrt{2B}}\left(\sqrt{m'}\delta_{m,m'-1} - \sqrt{m'+1}\delta_{m,m'+1}\right)\delta_{N,N'} + \frac{1}{\sqrt{2B}}\left(\sqrt{N'}\delta_{N,N'-1} + \sqrt{N'+1}\delta_{N,N'+1}\right)\delta_{m,m'}.\end{aligned}\quad (\text{A9})$$

The intra-Landau level matrix coordinates are then obtained as

$$\begin{aligned}(X^{(N)})_{mm'} &\equiv \langle N, m|x|N, m'\rangle = \frac{1}{\sqrt{2B}}\left(\sqrt{m'}\delta_{m,m'-1} + \sqrt{m'+1}\delta_{m,m'+1}\right), \\ (Y^{(N)})_{mm'} &\equiv \langle N, m|y|N, m'\rangle = -i\frac{1}{\sqrt{2B}}\left(\sqrt{m'}\delta_{m,m'-1} - \sqrt{m'+1}\delta_{m,m'+1}\right),\end{aligned}\quad (\text{A10})$$

or

$$X^{(N)} = \frac{1}{\sqrt{2B}} \begin{pmatrix} 0 & \sqrt{1} & 0 & 0 & 0 & 0 \\ \sqrt{1} & 0 & \sqrt{2} & 0 & 0 & 0 \\ 0 & \sqrt{2} & 0 & \sqrt{3} & 0 & 0 \\ 0 & 0 & \sqrt{3} & 0 & \ddots & 0 \\ 0 & 0 & 0 & \ddots & 0 & \ddots \end{pmatrix}, \quad Y^{(N)} = i\frac{1}{\sqrt{2B}} \begin{pmatrix} 0 & -\sqrt{1} & 0 & 0 & 0 & 0 \\ \sqrt{1} & 0 & -\sqrt{2} & 0 & 0 & 0 \\ 0 & \sqrt{2} & 0 & -\sqrt{3} & 0 & 0 \\ 0 & 0 & \sqrt{3} & 0 & \ddots & 0 \\ 0 & 0 & 0 & \ddots & 0 & \ddots \end{pmatrix}. \quad (\text{A11})$$

Notice that (A11) does not depend on the Landau level index  $N$ , and the matrix coordinates satisfy

$$[X^{(N)}, Y^{(N)}] = i\frac{1}{B}\mathbf{1}. \quad (\text{A12})$$

Obviously, the dimensionless coordinates,  $\hat{X}^{(N)} = \sqrt{B}X^{(N)}$  and  $\hat{Y}^{(N)} = \sqrt{B}Y^{(N)}$ , satisfy the Heisenberg-Weyl algebra together with  $\mathbf{1}$ :

$$[\hat{X}^{(N)}, \hat{Y}^{(N)}] = i\mathbf{1}, \quad [\hat{X}^{(N)}, \mathbf{1}] = [\hat{Y}^{(N)}, \mathbf{1}] = 0. \quad (\text{A13})$$

We have thus confirmed the emergence of the Groenewold-Moyal plane in any Landau level.

## APPENDIX B: TWO-SPHERE MATRIX COORDINATES IN YANG-MILLS MATRIX MODELS

For comparison with the fuzzy four-sphere (Sec. VII), we revisit the matrix model analyses of the fuzzy

two-sphere [101,102], clarifying physical properties of the matrix coordinates in the  $SO(3)$  Landau model.

### 1. Basic properties

The  $N$ th Landau level matrix coordinates  $X_i^{(N)}$  (8) satisfy the following relations:<sup>25</sup>

$$X_i^{(N)}X_i^{(N)} = c_1(N, I)\mathbf{1}_{D(N, I)}, \quad (\text{B1a})$$

$$X_j^{(N)}X_i^{(N)}X_j^{(N)} = c_2(N, I)X_i^{(N)}, \quad (\text{B1b})$$

$$\epsilon_{ijk}X_j^{(N)}X_k^{(N)} = 2ic_3(N, I)X_i^{(N)}, \quad (\text{B1c})$$

where

$$D(N, I) = I + 2N + 1, \quad (\text{B2})$$

<sup>25</sup>In the literatures on matrix models, it is common to denote the variables  $D$  and  $I$  as  $N$  and  $n$ , respectively.

and

$$c_1(N, I) \equiv \frac{I^2}{(I + 2N)(I + 2N + 2)}, \quad (\text{B3a})$$

$$c_2(N, I) \equiv \frac{I^2}{(I + 2N)^2(I + 2N + 2)^2} \times ((I + 2N)(I + 2N + 2) - 4), \quad (\text{B3b})$$

$$c_3(N, I) \equiv \frac{I}{(I + 2N)(I + 2N + 2)}. \quad (\text{B3c})$$

These  $c$ s are not independent quantities; instead, they satisfy

$$c_1 - c_2 = 4c_3^2. \quad (\text{B4})$$

From (B3), we readily have

$$-\frac{1}{4}[X_i^{(N)}, X_j^{(N)}]^2 = \frac{1}{2}(c_2 - c_2)c_1 \mathbf{1}_D \quad (\text{B5})$$

and

$$\begin{aligned} V(N, I) &= -\frac{1}{4} \text{tr}([X_i^{(N)}, X_j^{(N)}]^2) \\ &= \frac{1}{2}(c_2 - c_2)c_1 D \\ &= 2 \frac{I^4}{(I + 2N)^3(I + 2N + 2)^3} (2N + I + 1). \end{aligned} \quad (\text{B6})$$

The behaviors of (B3) and (B6) are shown in Fig. 16.

We introduce “normalized” matrix coordinates that satisfy the  $SU(2)$  algebra

$$[\hat{X}_i^{(N)}, \hat{X}_j^{(N)}] = 2i\epsilon_{ijk} \hat{X}_k^{(N)} \quad (\text{B7})$$

as

$$\hat{X}_i^{(N)} = \frac{1}{c_3(N, I)} X_i^{(N)} = 2S_i^{(\frac{l}{2}+N)}. \quad (\text{B8})$$

Notice that  $\hat{X}_i^{(N)}$  depend on the  $SU(2)$  index  $l = N + \frac{1}{2}$  rather than  $N$  and  $I$ , separately. Several important physical quantities are evaluated as

$$\text{radius: } \hat{R} = \frac{\sqrt{c_1}}{c_3} = \sqrt{(I + 2N)(I + 2N + 2)}, \quad (\text{B9a})$$

$$\text{potential energy: } V = -\frac{1}{4} \text{tr}([\hat{X}_i^{(N)}, \hat{X}_j^{(N)}]^2) = \frac{2}{c_3^2} c_1 D(N, I) = 2(I + 2N)(I + 2N + 1)(I + 2N + 2), \quad (\text{B9b})$$

$$\text{potential energy density: } \frac{V}{\hat{R}^2} = 2D(N, I) = 2(I + 2N + 1). \quad (\text{B9c})$$

The potential energy density is simply the twice the matrix size of the fuzzy two-sphere.

## 2. Matrix model analysis

Yang-Mills matrix models with a mass term and with a third-rank Chern-Simons term are given by

$$\begin{aligned} S_{\text{mass}} &= -\frac{1}{4} \text{tr}([A_i, A_j]^2) - \frac{1}{2} \text{tr}(A_i^2), \\ S_{\text{CS}} &= -\frac{1}{4} \text{tr}([A_i, A_j]^2) + i\frac{1}{3} \epsilon_{ijk} \text{tr}(A_i A_j A_k), \end{aligned} \quad (\text{B10})$$

and the corresponding equations of motion are, respectively,

$$[[A_i, A_j], A_j] = A_i, \quad [[A_i, A_j], A_i] = -i\epsilon_{ijk} A_j A_k, \quad (\text{B11})$$

The fuzzy two-sphere is realized as a solution:

$$A_i^{\text{cl}} = \alpha_{\text{mass}} \hat{X}_i^{(N)}, \quad A_i^{\text{cl}} = \alpha_{\text{CS}} \hat{X}_i^{(N)}, \quad (\text{B12})$$

with

$$\alpha_{\text{mass}} \equiv \frac{1}{2\sqrt{2}}, \quad \alpha_{\text{CS}} \equiv \frac{1}{4}. \quad (\text{B13})$$

Notice that both coefficients,  $\alpha_{\text{mass}}$  and  $\alpha_{\text{CS}}$ , are constant unlike the case of the fuzzy four-sphere solutions (see Sec. VII). The classical solutions (B12) have the following properties:

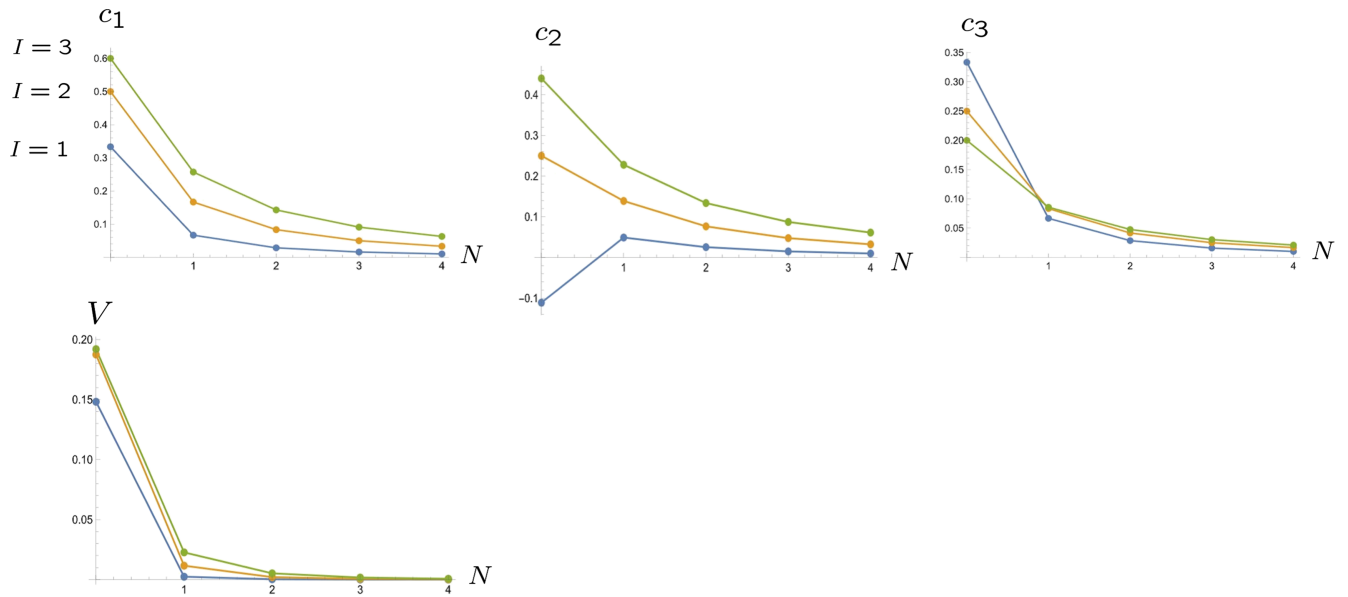


FIG. 16. The blue, orange, and green lines correspond to  $I = 1, 2, 3$  of Eqs. (B3) and (B6).

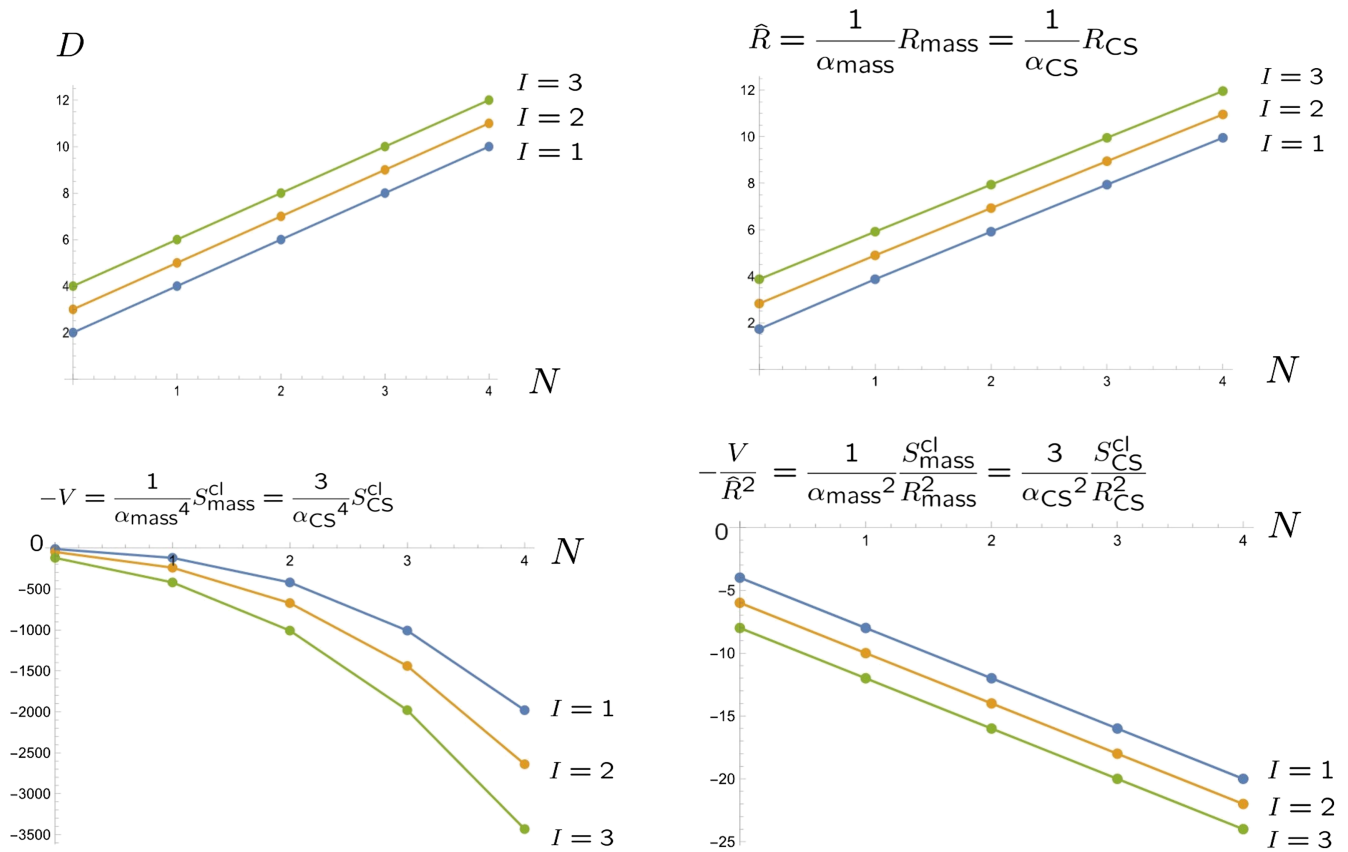


FIG. 17. Physical quantities of the fuzzy two-spheres. All quantities monotonically increase or decrease as  $N$  and  $I$  increase.

$$\text{radius: } R_{\text{mass}} \equiv \alpha_{\text{mass}} \hat{R} \quad (A_i^{\text{cl}} A_i^{\text{cl}} = R_{\text{mass}}^2 \mathbf{1}), \quad R_{\text{CS}} \equiv \alpha_{\text{CS}} \hat{R} \quad (A_i^{\text{cl}} A_i^{\text{cl}} = R_{\text{CS}}^2 \mathbf{1}), \quad (\text{B14a})$$

$$\text{action: } S_{\text{mass}}^{\text{cl}} = \overbrace{\left(-\frac{1}{4} + \frac{1}{2}\right)}{=1/4} \text{tr}([A_i^{\text{cl}}, A_i^{\text{cl}}]^2) = -\alpha_{\text{mass}}^4 V, \quad S_{\text{CS}}^{\text{cl}} \equiv S_{\text{CS}}[A_i^{\text{cl}}] = \overbrace{\left(-\frac{1}{4} + \frac{1}{3}\right)}{=1/12} \text{tr}([A_i^{\text{cl}}, A_j^{\text{cl}}]^2) = -\frac{1}{3} \alpha_{\text{CS}}^4 V, \quad (\text{B14b})$$

$$\text{action density: } \frac{S_{\text{mass}}^{\text{cl}}}{R_{\text{mass}}^2} = -\alpha_{\text{mass}}^2 \frac{V}{\hat{R}^2} = -\frac{1}{4} D, \quad \frac{S_{\text{CS}}^{\text{cl}}}{R_{\text{CS}}^2} = -\frac{1}{3} \alpha_{\text{CS}}^2 \frac{V}{\hat{R}^2} = -\frac{1}{24} D. \quad (\text{B14c})$$

See Fig. 17 for the behaviors of these quantities.

- 
- [1] Hartland S. Snyder, Quantized space-time, *Phys. Rev.* **71**, 38 (1947).
- [2] C. N. Yang, On quantized space-time, *Phys. Rev.* **72**, 874 (1947).
- [3] Miao Li and Yong-Shi Wu, *Physics in Noncommutative World: Field Theories* (Rinton Press, Princeton, New Jersey, 2002).
- [4] Alain Connes, *Noncommutative Geometry* (Academic Press, New York, 1994).
- [5] S. Twareque Ali and Miroslav Engliš, Quantization methods: A guide for physicists and analysts, *Rev. Math. Phys.* **17**, 391 (2005).
- [6] Thomas L. Curtright and Cosmas K. Zachos, Quantum mechanics in Phase Space, *Asia Pac. Phys. Newsl.* **1**, 37 (2012).
- [7] Cosmas K. Zachos, David B. Fairlie, and Thomas L. Curtright, *Quantum Mechanics in Phase Space* (World Scientific Pub. Co. Inc., Singapore, 2006).
- [8] Anirban Basu and Jeffrey A. Harvey, The M2-M5 brane system and a generalized Nahm's equation, *Nucl. Phys.* **B713**, 136 (2005).
- [9] Jonathan Bagger and Neil Lambert, Modeling multiple M2's, *Phys. Rev. D* **75**, 045020 (2007).
- [10] Andreas Gustavsson, Algebraic structures on parallel M2-branes, *Nucl. Phys.* **B 811**, 66 (2009).
- [11] Jonathan Bagger and Neil Lambert, Gauge symmetry and supersymmetry of multiple M2-branes, *Phys. Rev. D* **77**, 065008 (2008).
- [12] T. Banks, W. Fischler, S. Shenker, and L. Susskind, M theory as a matrix model: A conjecture, *Phys. Rev. D* **55**, 5112 (1997).
- [13] N. Ishibashi, H. Kawai, Y. Kitazawa, and A. Tsuchiya, A large N reduced model as super-string, *Nucl. Phys.* **B498**, 467 (1997).
- [14] J. Madore, The fuzzy sphere, *Classical Quantum Gravity* **9**, 69 (1992).
- [15] H. Grosse, C. Klimcik, and P. Presnajder, On finite 4D quantum field theory in non-commutative geometry, *Commun. Math. Phys.* **180**, 429 (1996).
- [16] Judith Castelino, Sangmin Lee, and Washington Taylor, Longitudinal 5-branes as 4-spheres in matrix theory, *Nucl. Phys.* **B526**, 334 (1998).
- [17] H. Grosse and G. Reiter, The fuzzy supersphere, *J. Geom. Phys.* **28**, 349 (1998).
- [18] Z. Guralnik and S. Ramgoolam, On the polarization of unstable D0-branes into non-commutative odd spheres, *J. High Energy Phys.* **02** (2001) 032.
- [19] G. Alexanian, A. P. Balachandran, G. Immirzi, and B. Ydri, Fuzzy CP2, *J. Geom. Phys.* **42**, 28 (2002).
- [20] P. M. Ho and S. Ramgoolam, Higher dimensional geometries from matrix brane constructions, *Nucl. Phys.* **B627**, 266 (2002).
- [21] Sanjaye Ramgoolam, Higher dimensional geometries related to fuzzy odd-dimensional spheres, *J. High Energy Phys.* **10** (2002) 064.
- [22] Yusuke Kimura, On higher dimensional fuzzy spherical branes, *Nucl. Phys.* **B664**, 512 (2003).
- [23] M. M. Sheikh-Jabbari, Tiny graviton matrix theory: DLCQ of IIB plane-wave string theory, a conjecture, *J. High Energy Phys.* **09** (2004) 017.
- [24] Joakim Arnlind, Martin Bordemann, Laurent Hofer, Jens Hoppe, and Hidehiko Shimada, Fuzzy Riemann surfaces, *J. High Energy Phys.* **06** (2009) 047.
- [25] Kazuki Hasebe, Graded Hopf maps and fuzzy superspheres, *Nucl. Phys.* **B853**, 777 (2011).
- [26] Kazuki Hasebe, Non-compact Hopf maps and fuzzy ultra-hyperboloids, *Nucl. Phys.* **B865**, 148 (2012).
- [27] Washington Taylor, The M(atrrix) model of M-theory, [arXiv:hep-th/0002016](https://arxiv.org/abs/hep-th/0002016).
- [28] Washington Taylor, M(atrrix) theory: Matrix quantum mechanics as a fundamental theory, *Rev. Mod. Phys.* **73**, 419 (2001).
- [29] Yoichiro Nambu, Generalized Hamiltonian dynamics, *Phys. Rev. D* **7**, 2405 (1973).
- [30] Pei-Ming Ho and Yutaka Matsuo, Nambu bracket and M-theory, *Prog. Theor. Exp. Phys.* **2016**, 06A104 (2016).
- [31] Thomas Curtright and Cosmas Zachos, Classical and quantum Nambu mechanics, *Phys. Rev. D* **68**, 085001 (2003).

- [32] Joshua DeBellis, Christian Saemann, and Richard J. Szabo, Quantized Nambu-Poisson manifolds and  $n$ -Lie algebras, *J. Math. Phys. (N.Y.)* **51**, 122303 (2010).
- [33] Y. Kawamura, Cubic matrices, generalized spin algebra and uncertainty relation, *Prog. Theor. Phys.* **110**, 579 (2003).
- [34] Y. Kawamura, Dynamical theory of generalized matrices, *Prog. Theor. Phys.* **114**, 669 (2005).
- [35] Pei-Ming Ho, Ru-Chuen Hou, and Yutaka Matsuo, Lie 3-algebra and multiple M2-branes, *J. High Energy Phys.* **06** (2008) 020.
- [36] Leon Takhtajan, On foundation of the generalized Nambu mechanics, *Commun. Math. Phys.* **160**, 295 (1994).
- [37] Giuseppe Dito, Moshe Flato, Daniel Sternheimer, and Leon Takhtajan, Deformation quantization and Nambu mechanics, *Commun. Math. Phys.* **183**, 1 (1997).
- [38] Giuseppe Dito and Moshe Flato, Generalized Abelian deformations: Application to Nambu mechanics, *Lett. Math. Phys.* **39**, 107 (1997).
- [39] Kazuki Hasebe, Hopf maps, lowest Landau level, and fuzzy spheres, *SIGMA* **6**, 071 (2010).
- [40] Dimitra Karabali, V.P. Nair, and S. Randjbar-Daemi, Fuzzy spaces, the M(atr)ix model and the quantum Hall effect, [arXiv:hep-th/0407007](https://arxiv.org/abs/hep-th/0407007).
- [41] S. C. Zhang and J. P. Hu, A four dimensional generalization of the quantum Hall effect, *Science* **294**, 823 (2001).
- [42] Dimitra Karabali and V. P. Nair, Quantum Hall effect in higher dimensions, *Nucl. Phys.* **B641**, 533 (2002).
- [43] B. A. Bernevig, J. P. Hu, N. Toumbas, and S. C. Zhang, The eight dimensional quantum Hall effect and the octonions, *Phys. Rev. Lett.* **91**, 236803 (2003).
- [44] K. Hasebe and Y. Kimura, Dimensional hierarchy in quantum Hall effects on fuzzy spheres, *Phys. Lett. B* **602**, 255 (2004).
- [45] K. Hasebe, Supersymmetric quantum Hall effect on fuzzy supersphere, *Phys. Rev. Lett.* **94**, 206802 (2005).
- [46] V. P. Nair and S. Randjbar-Daemi, Quantum Hall effect on  $S^3$ , edge states and fuzzy  $S^3/\mathbb{Z}_2$ , *Nucl. Phys.* **B679**, 447 (2004).
- [47] A. Jellal, Quantum Hall effect on higher dimensional spaces, *Nucl. Phys.* **B725**, 554 (2005).
- [48] Kazuki Hasebe, Split-quaternionic Hopf map, quantum Hall effect, and twistor theory, *Phys. Rev. D* **81**, 041702 (2010).
- [49] F. Balli, A. Behtash, S. Kurkcuglu, and G. Unal, Quantum Hall effect on the Grassmannians  $Gr_2(C^N)$ , *Phys. Rev. D* **89**, 105031 (2014).
- [50] Kazuki Hasebe, Chiral topological insulator on Nambu 3-algebraic geometry, *Nucl. Phys.* **B886**, 681 (2014).
- [51] U. H. Coskun, S. Kurkcuglu, and G. C. Toga, Quantum Hall effect on odd spheres, *Phys. Rev. D* **95**, 065021 (2017).
- [52] Jonathan J. Heckman and Luigi Tizzano, 6D fractional quantum Hall effect, *J. High Energy Phys.* **05** (2018) 120.
- [53] Kazuki Hasebe, Relativistic Landau models and generation of fuzzy spheres, *Int. J. Mod. Phys. A* **31**, 1650117 (2016).
- [54] Kazuki Hasebe,  $SO(4)$  Landau models and matrix geometry, *Nucl. Phys.* **B934**, 149 (2018).
- [55] Kazuki Hasebe,  $SO(5)$  Landau models and nested Nambu matrix geometry, *Nucl. Phys.* **B956**, 115012 (2020).
- [56] Kazuki Hasebe,  $SO(5)$  Landau model and 4D quantum Hall effect in the  $SO(4)$  monopole background, *Phys. Rev. D* **105**, 065010 (2022).
- [57] Kazuki Hasebe, Quantum matrix geometry in the lowest Landau level and higher Landau levels, *Proc. Sci. CORFU2021* (2022) 239.
- [58] Goro Ishiki, Takaki Matsumoto, and Hisayoshi Muraki, Kähler structure in the commutative limit of matrix geometry, *J. High Energy Phys.* **08** (2016) 042.
- [59] Tsuguhiko Asakawa, Goro Ishiki, Takaki Matsumoto, So Matsuura, and Hisayoshi Muraki, Commutative geometry for non-commutative D-branes by tachyon condensation, *Prog. Theor. Exp. Phys.* **2018**, 063B04 (2018).
- [60] G. Ishiki, T. Matsumoto, and H. Muraki, Information metric, Berry connection, and Berezin-Toeplitz quantization for matrix geometry, *Phys. Rev. D* **98**, 026002 (2018).
- [61] Kaho Matsuura and Asato Tsuchiya, Matrix geometry for ellipsoids, *Prog. Theor. Exp. Phys.* **2020**, 033B05 (2020).
- [62] V. P. Nair, Landau-Hall states and Berezin-Toeplitz quantization of matrix algebras, *Phys. Rev. D* **102**, 025015 (2020).
- [63] Hiroyuki Adachi, Goro Ishiki, Takaki Matsumoto, and Kaishu Saito, The matrix regularization for Riemann surfaces with magnetic fluxes, *Phys. Rev. D* **101**, 106009 (2020).
- [64] Hiroyuki Adachi, Goro Ishiki, and Satoshi Kanno, Vector bundles on fuzzy Kähler manifolds, [arXiv:2210.01397](https://arxiv.org/abs/2210.01397).
- [65] H. M. Price, O. Zilberberg, T. Ozawa, I. Carusotto, and N. Goldman, Four-dimensional quantum Hall effect with ultracold atoms, *Phys. Rev. Lett.* **115**, 195303 (2015).
- [66] H. M. Price, O. Zilberberg, T. Ozawa, I. Carusotto, and N. Goldman, Measurement of Chern numbers through center-of-mass responses, *Phys. Rev. B* **93**, 245113 (2016).
- [67] T. Ozawa, H. M. Price, N. Goldman, O. Zilberberg, and I. Carusotto, Synthetic dimensions in integrated photonics: From optical isolation to four-dimensional quantum Hall physics, *Phys. Rev. A* **93**, 043827 (2016).
- [68] Shaojie Ma, Hongwei Jia, Yangang Bi, Shangqiang Ning, Fuxin Guan, Hongchao Liu, Chenjie Wang, and Shuang Zhang, Gauge field induced chiral zero mode in five-dimensional Yang monopole metamaterials, *Phys. Rev. Lett.* **130**, 243801 (2023).
- [69] Xingen Zheng, Tian Chen, Weixuan Zhang, Houjun Sun, and Xiangdong Zhang, Exploring topological phase transition and Weyl physics in five dimensions with electric circuits, *Phys. Rev. Res.* **4**, 033203 (2022).
- [70] Sh. Ma, Y. Bi, Q. Guo, B. Yang, O. You, J. Feng, H.-B. Sun, and Sh. Zhang, Linked Weyl surfaces and Weyl arcs in photonic metamaterials, *Science* **373**, 572 (2021).
- [71] S. Sugawa, F. Salces-Carcoba, A. R. Perry, Y. Yue, and I. B. Spielman, Second Chern number of a quantum-simulated non-Abelian Yang monopole, *Science* **360**, 1429 (2018).
- [72] T. T. Wu and C. N. Yang, Dirac monopoles without strings: Monopole harmonics, *Nucl. Phys.* **B107**, 1030 (1976).

- [73] F. D. M. Haldane, Fractional quantization of the Hall effect: A hierarchy of incompressible quantum fluid states, *Phys. Rev. Lett.* **51**, 605 (1983).
- [74] Mikio Nakahara, *Geometry, Topology and Physics*, 2nd ed., Graduate Student Series in Physics (Institute of Physics, Bristol, 2003).
- [75] Kazuki Hasebe, Higher dimensional quantum Hall effect as A-class topological insulator, *Nucl. Phys.* **B886**, 952 (2014).
- [76] Shou-Cheng Zhang, To see a world in a grain of sand, A chapter for John Wheeler's 90's birthday festschrift, [arXiv: hep-th/0210162](https://arxiv.org/abs/hep-th/0210162).
- [77] Martin Schlichenmaier, Berezin-Toeplitz quantization and Berezin transform, in *Long Time Behaviour of Classical and Quantum Systems (Proceedings of the Bologna APTEX International Conference)*, edited by Sandro Graffi and André Martinez (World Scientific Publishing, Singapore, 2001), pp. 271–287, [arXiv:math/0009219](https://arxiv.org/abs/math/0009219).
- [78] Yuri A. Kordyukov, Berezin-Toeplitz quantization associated with higher Landau levels of the Bochner Laplacian, [arXiv:2012.14198](https://arxiv.org/abs/2012.14198).
- [79] Laurent Charles, Landau levels on a compact manifold, [arXiv:2012.14190](https://arxiv.org/abs/2012.14190).
- [80] Chen Ning Yang, Generalization of Dirac's monopole to SU2 gauge fields, *J. Math. Phys. (N.Y.)* **19**, 320 (1978).
- [81] Chen Ning Yang, SU(2) monopole harmonics, *J. Math. Phys. (N.Y.)* **19**, 2622 (1978).
- [82] Kazuki Hasebe, Generating quantum matrix geometry from gauged quantum mechanics, [arXiv:2310.01051](https://arxiv.org/abs/2310.01051).
- [83] Yasuhiro Abe, Construction of fuzzy  $S^4$ , *Phys. Rev. D* **70**, 126004 (2004).
- [84] Robert C. Myers, Dielectric-branes, *J. High Energy Phys.* **12** (1999) 022.
- [85] Marcus Sperling and Harold C. Steinacker, Covariant 4-dimensional fuzzy spheres, matrix models and higher spin, *J. Phys. A* **50**, 375202 (2017).
- [86] Harold Steinacker, One-loop stabilization of the fuzzy four-sphere via softly broken SUSY, *J. High Energy Phys.* **12** (2015) 115.
- [87] Harald Grosse and Harold Steinacker, Finite gauge theory on fuzzy  $CP^2$ , *Nucl. Phys.* **B707**, 145 (2005).
- [88] Goro Ishiki, Matrix geometry and coherent states, *Phys. Rev. D* **92**, 046009 (2015).
- [89] Lukas Schneiderbauer and Harold C. Steinacker, Measuring finite quantum geometries via quasi-coherent states, *J. Phys. A* **49**, 285301 (2016).
- [90] Harold C. Steinacker, Quantum (matrix) geometry and quasi-coherent states, *J. Phys. A* **54**, 055401 (2021).
- [91] David Berenstein and Eric Dzienkowski, Matrix embeddings on flat  $\mathbb{R}^3$  and the geometry of membranes, *Phys. Rev. D* **86**, 086001 (2012).
- [92] Joanna L. Karczmarek and Ken Huai-Che Yeh, Noncommutative spaces and matrix embeddings on flat  $\mathbb{R}^{2n+1}$ , *J. High Energy Phys.* **11** (2015) 146.
- [93] Mathias Hudoba de Badyn, Joanna L. Karczmarek, Philippe Sabella-Garnier, and Ken Huai-Che Yeh, Emergent geometry of membranes, *J. High Energy Phys.* **11** (2015) 089.
- [94] Kazuki Hasebe (to be published).
- [95] Yusuke Kimura, Noncommutative gauge theory on fuzzy four-sphere and matrix model, *Nucl. Phys.* **B637**, 177 (2002).
- [96] Kazuki Hasebe, Higher (odd) dimensional quantum Hall effect and extended dimensional hierarchy, *Nucl. Phys.* **B920**, 475 (2017).
- [97] Tsuguhiko Asakawa, Shigeki Sugimoto, and Seiji Terashima, Exact description of D-branes via tachyon condensation, *J. High Energy Phys.* **02** (2003) 011.
- [98] Seiji Terashima, Noncommutativity and tachyon condensation, *J. High Energy Phys.* **10** (2005) 043.
- [99] Anton Kapustin and Lev Spodyneiko, Higher-dimensional generalizations of Berry curvature, *Phys. Rev. B* **101**, 235130 (2020).
- [100] A. Kitaev, Differential forms on the space of statistical mechanical lattice models, in *Talk at Between Topology and Quantum Field Theory: A Conference in Celebration of Dan Freed's 60th birthday*, <https://web.ma.utexas.edu/topqft/talkslides/kitaev.pdf>.
- [101] Yusuke Kimura, Noncommutative gauge theories on fuzzy sphere and fuzzy torus from matrix model, *Prog. Theor. Phys.* **106**, 445 (2001).
- [102] Satoshi Iso, Yusuke Kimura, Kenji Tanaka, and Kazunori Wakatsuki, Noncommutative gauge theory on fuzzy sphere from matrix model, *Nucl. Phys.* **B604**, 121 (2001).